

SUPPORTING INFORMATION

Centrally Active Multitarget Anti-Alzheimer Agents Derived from the Antioxidant Lead CR-6

F. Javier Pérez-Areales,[†] María Garrido,[‡] Ester Aso,[§] Manuela Bartolini,[△] Angela De Simone,[¶] Alba Espargaró,[#] Tiziana Ginex,[⊥] Raimon Sabate,[#] Belén Pérez,^{||} Vincenza Andrisano,[▽] Dolors Puigoriol-Illamola,^{} Mercè Pallàs,^{*} F. Javier Luque,[⊥] María Isabel Loza,[◇] José Brea,[◇] Isidro Ferrer,^{§,◊} Francisco Ciruela,[§] Angel Messeguer,[‡] Diego Muñoz-Torrero^{*,}*

^{*}Laboratory of Pharmaceutical Chemistry (CSIC Associated Unit), Faculty of Pharmacy and Food Sciences, and Institute of Biomedicine (IBUB), University of Barcelona (UB), E-08028
Barcelona, Spain

[†]Department of Biological Chemistry, Institute of Advanced Chemistry of Catalonia (IQAC-CSIC), E-08034 Barcelona, Spain

[§] Department of Pathology and Experimental Therapeutics, Neurosciences Institute, UB, and Bellvitge University Hospital - IDIBELL, E-08908 L'Hospitalet de Llobregat, Spain

[△]Department of Pharmacy and Biotechnology, University of Bologna, I-40126 Bologna, Italy

[¶]Department of Drug Science and Technology, University of Turin, I-10125 Torino, Italy

[#]Department of Pharmacy, Pharmaceutical Technology and Physical-Chemistry, Faculty of Pharmacy and Food Sciences, and Institute of Nanoscience and Nanotechnology (IN2UB), UB, E-08028 Barcelona, Spain

[†]Department of Nutrition, Food Science and Gastronomy, Faculty of Pharmacy and Food Sciences, IBUB, and Institute of Theoretical and Computational Chemistry (IQTc), UB, E-08921 Santa Coloma de Gramenet, Spain

^{||}Department of Pharmacology, Therapeutics, and Toxicology, Autonomous University of Barcelona, E-08193 Bellaterra, Spain

[▼]Department for Life Quality Studies, University of Bologna, I-47921 Rimini, Italy

[◆]Pharmacology Section, Department of Pharmacology, Toxicology and Therapeutic Chemistry, Faculty of Pharmacy and Food Sciences, and Institute of Neuroscience (NeuroUB), UB, E-08028 Barcelona, Spain

[□]BioFarma Research Group, Centro Singular de Investigación en Medicina Molecular y Enfermedades Crónicas (CIMUS), Universidade de Santiago de Compostela, Av. de Barcelona s/n, E-15782, Santiago de Compostela, Spain

[◊]CIBERNED, E-28031 Madrid, Spain

TABLE OF CONTENTS

Figure S1. RMSD analysis of protein backbone, heavy atoms and residues in the binding site of hAChE bound to (*R*)-**6b** and (*S*)-**6b**

S4

Figure S2. MD-averaged (<i>R</i>)- 6b -hBChE and (<i>S</i>)- 6b -hBChE complexes	S5
Figure S3. RMSD analysis of protein backbone, heavy atoms and residues in the binding site of hBChE bound to (<i>R</i>)- 6b and (<i>S</i>)- 6b	S6
Figure S4. RMSD analysis of protein backbone, heavy atoms and residues in the binding site of hBChE bound to (<i>R</i>)- 12a and (<i>S</i>)- 12a	S7
Table S1. Results of commercial drugs for PAMPA-BBB assay validation	S8
Table S2. Antibodies used in Western blot studies	S9
Table S3. Primers used in qPCR studies	S9
Table S4. Relative MS peak areas in the identification of metabolites in human, mouse, and rat liver microsomes	S10
Figure S5. Binding mode of compounds 6b and 11b and the <i>p</i> -benzoquinone metabolite of 4b within hAChE	S11
Copies of ¹ H and ¹³ C NMR spectra and HPLC chromatograms of target compounds	S12

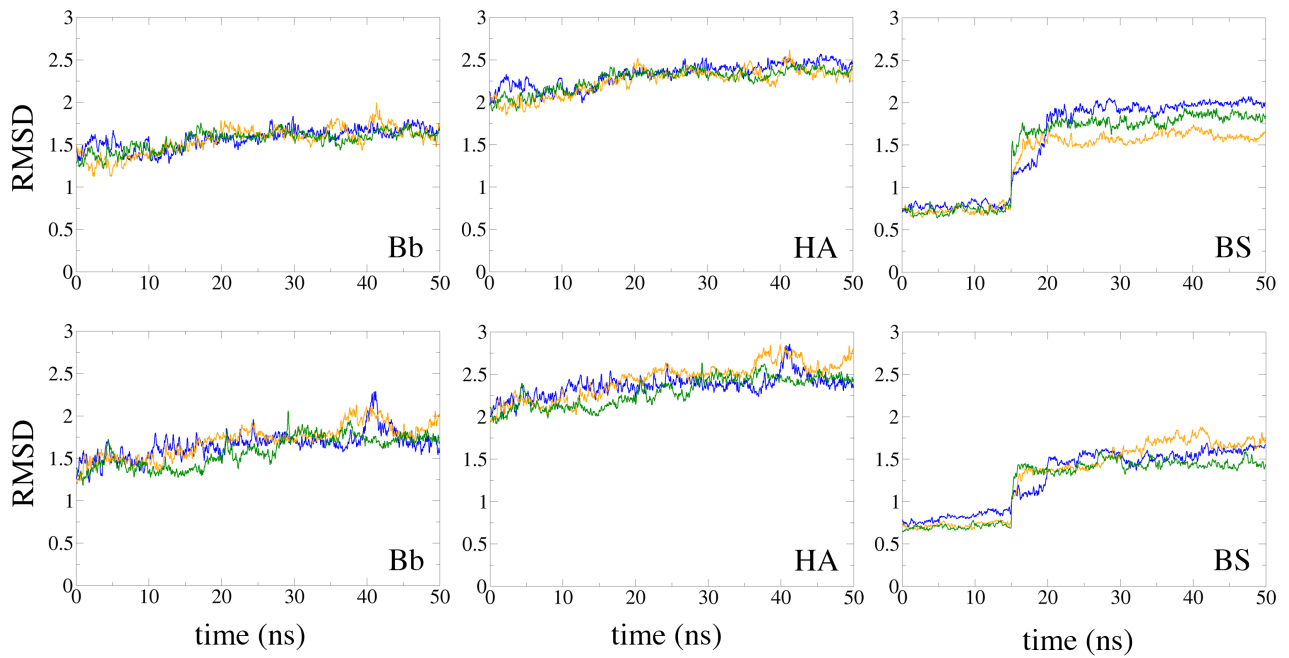


Figure S1. RMSD analysis of protein backbone (Bb), heavy atoms (HA) and residues in the binding site (BS) for the three independent MD simulations run for (*top*) (*R*)-**6b** and (*bottom*) (*S*)-**6b** bound to hAChE.

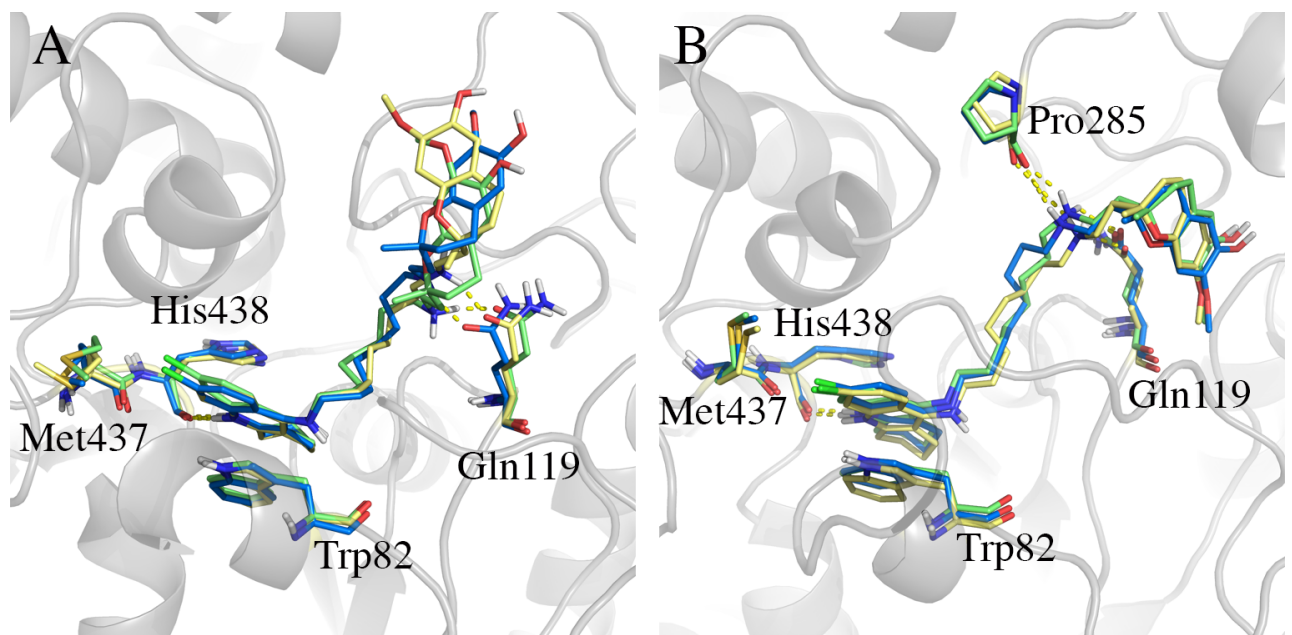


Figure S2. Protein–ligand complexes for (A) (*R*)-**6b** (A) and (B) (*S*)-**6b** bound to hBChE. MD-averaged complexes derived from three independent replicas run for each enantiomer are shown. Selected interactions are shown as yellow dashed lines.

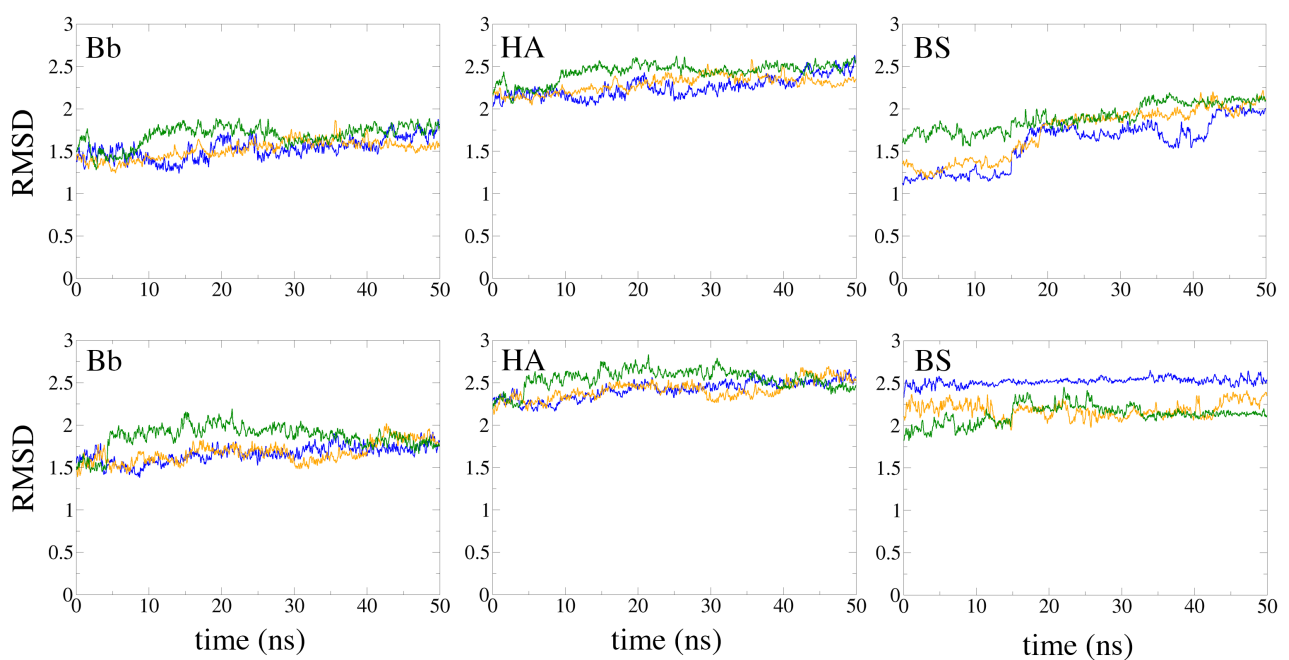


Figure S3. RMSD analysis of protein backbone (Bb), heavy atoms (HA) and residues in the binding site (BS) for the three independent MD simulations run for (*top*) (*R*)-**6b** and (*bottom*) (*S*)-**6b** bound to hBChE.

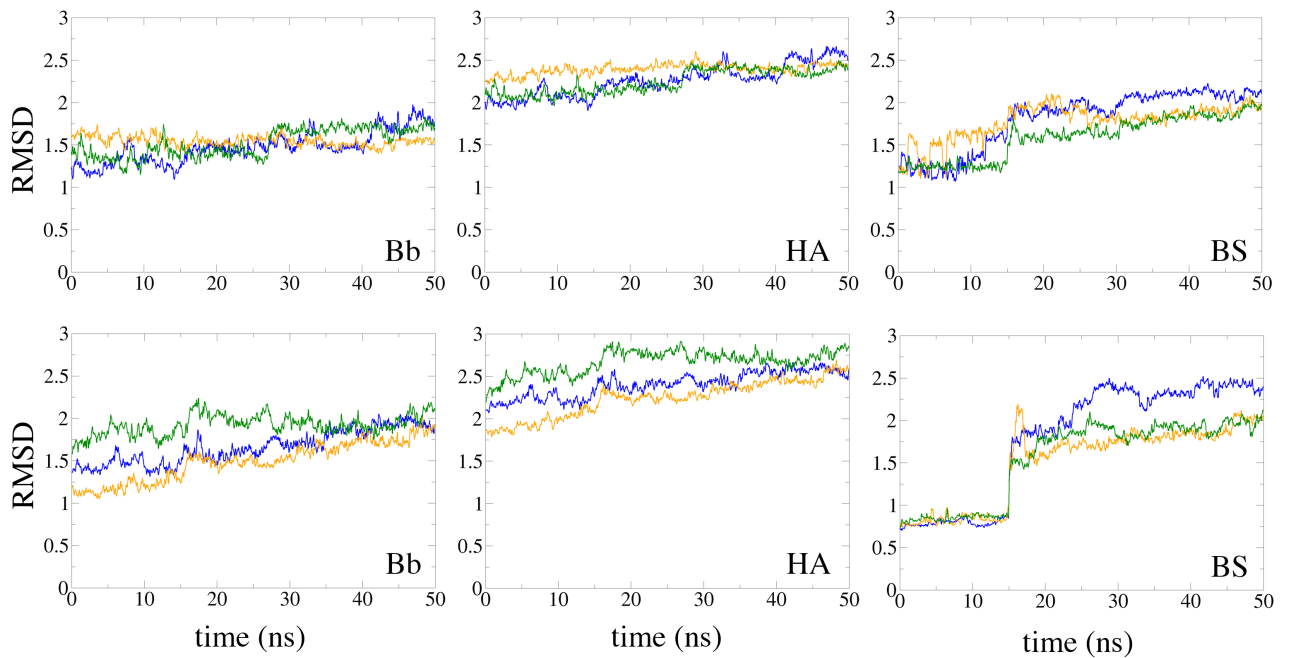


Figure S4. RMSD analysis of protein backbone (Bb), heavy atoms (HA) and residues in the binding site (BS) for the three independent MD simulations run for (*top*) (*R*)-**12a** and (*bottom*) (*S*)-**12a** bound to hBChE.

Table S1. Reported and Experimental Permeability (Pe 10^{-6} cm s $^{-1}$) Values in the PAMPA-BBB Assay of 14 Commercial Drugs Used for Assay Validation.

Compound	Bibliography value ^a	Experimental value (n=3) ± S.D.
Cimetidine	0.0	0.7 ± 0.1
Lomefloxacin	1.1	0.7 ± 0.1
Norfloxacin	0.1	0.9 ± 0.1
Ofloxacin	0.8	0.9 ± 0.1
Hydrocortisone	1.9	1.4 ± 0.1
Piroxicam	2.5	2.1 ± 0.1
Clonidine	5.3	6.5 ± 0.1
Corticosterone	5.1	6.7 ± 0.1
Imipramine	13.0	12.3 ± 0.1
Promazine	8.8	13.8 ± 0.3
Progesterone	9.3	16.8 ± 0.3
Desipramine	12.0	17.8 ± 0.1
Testosterone	17.0	25.6 ± 0.4
Verapamil	16.0	27.6 ± 0.5

^a Taken from Di, L.; Kerns, E. H.; Fan, K.; McConnell, O. J.; Carter, G. T. High throughput artificial membrane permeability assay for blood-brain barrier. *Eur. J. Med. Chem.* **2003**, *38*, 223–232.

Table S2. Antibodies Used in Western Blot Studies.

Antibody	Host	Source/Catalog	WB dilution
ADAM10	Rabbit	Abcam	1:1000
BACE1	Rabbit	Abcam	1:1000
sAPPα	Rabbit	Covance	1:2000
sAPPβ	Rabbit	Covance	1:2000
NRF2	Rabbit	Cell Signaling	1:1000
Catalase	Rabbit	Abcam	1:1000
GPX1	Rabbit	Novus Biological	1:2000
GAPDH	Mouse	Millipore	1:5000

Table S3. Primers Used in qPCR Studies.

Target	Product size (bp)	Forward primer (5'-3')	Reverse primer (5'-3')
<i>Adam10</i>	54	GGGAAGAAATGCAAGCTGAA	CTGTACAGCAGGGTCTTGAC
<i>Bace1</i>	128	AAGCTGCCGTCAAGTCCATC	GCGGAAGGACTGATTGGTGA
<i>Hmox1</i>	137	TGACACCTGAGGTCAAGCAC	GTCTCTGCAGGGGCAGTATC
<i>iNOS</i>	149	GAAGCGTTCGGGATCTGAA	GAAGCGTTCGGGATCTGAA
<i>Actin</i>	190	CAACGAGCGGTTCCGAT	GCCACAGGTTCCATAACCA

Table S4. Relative MS Peak Areas in the Identification of Metabolites in Human, Mouse, and Rat Liver Microsomes.^a

	4b	M1-M2	M3	M4
HLM 60 min	857.611	2,642.590	2,220.529	1,103.357
HLM 40 min	5,207.464	6,172.992	7,965.484	732.660
HLM 20 min	35,515.574	4,020.527	4,858.155	291.824
HLM 10 min	45,318.645	2,091.129	2,030.786	248.183
HLM 0 min	49,641.340	1,155.693	452.668	183.363
MLM 60 min	30,259.844	2,589.753	3,069.414	255.269
MLM 40 min	42,688.520	2,559.730	1,906.893	261.439
MLM 20 min	49,374.652	1,572.661	834.982	185.967
MLM 10 min	50,930.750	1,269.113	596.771	184.181
MLM 0 min	48,678.672	1,115.285	386.902	159.195
RLM 60 min	16,605.932	5,805.929	6,085.236	375.713
RLM 40 min	30,782.176	5,457.648	5,528.240	317.334
RLM 20 min	45,931.359	2,319.008	1,858.295	205.586
RLM 10 min	48,575.387	1,495.265	798.099	211.890
RLM 0 min	46,383.352	^b	449.619	140.174

^a HLM, human liver microsomes; MLM, mouse liver microsomes; RLM, rat liver microsomes. Values are expressed as the mean of two independent experiments, each performed in triplicate. ^b Area under the limit of detection.

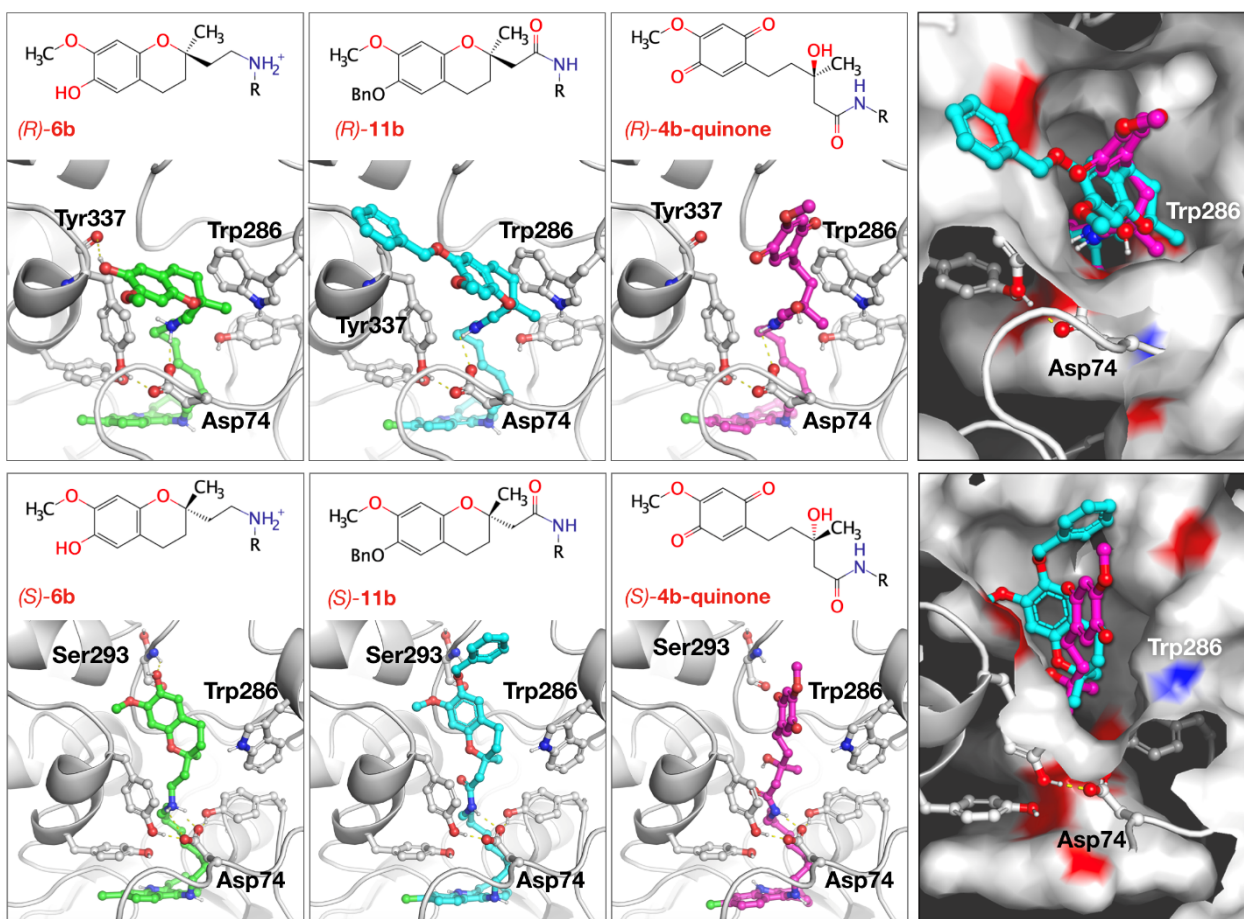
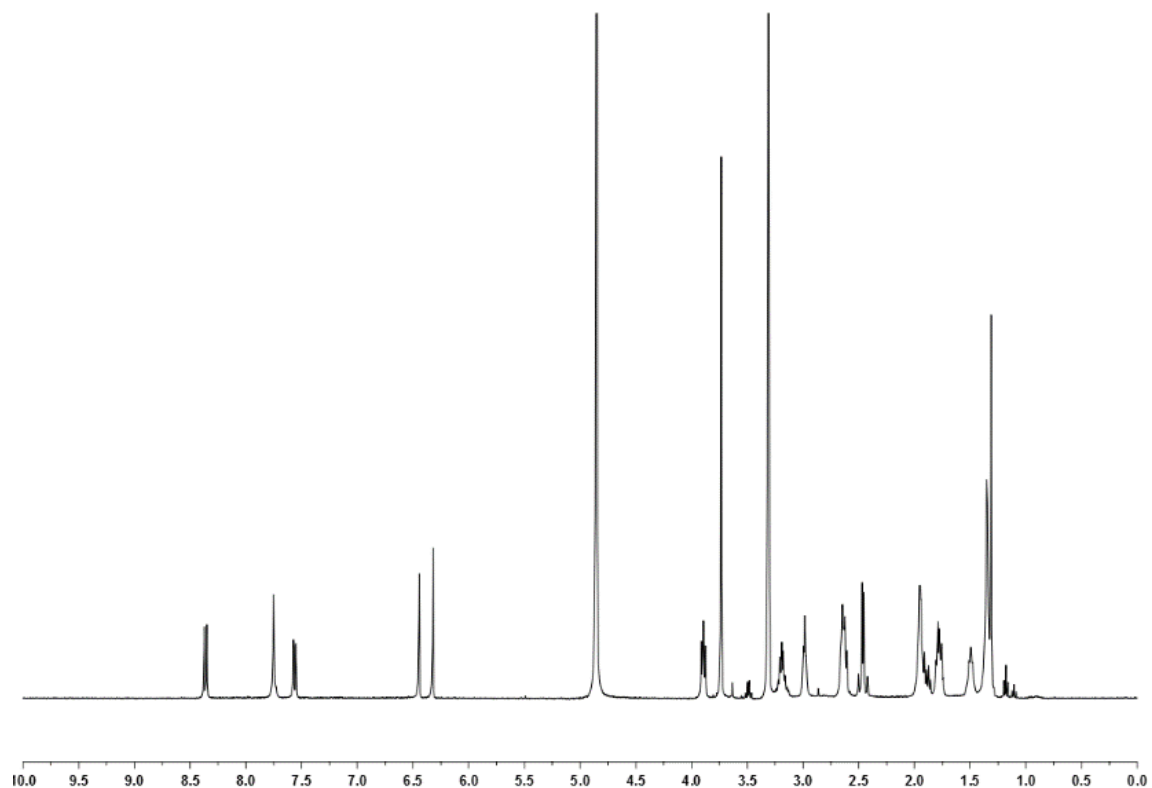
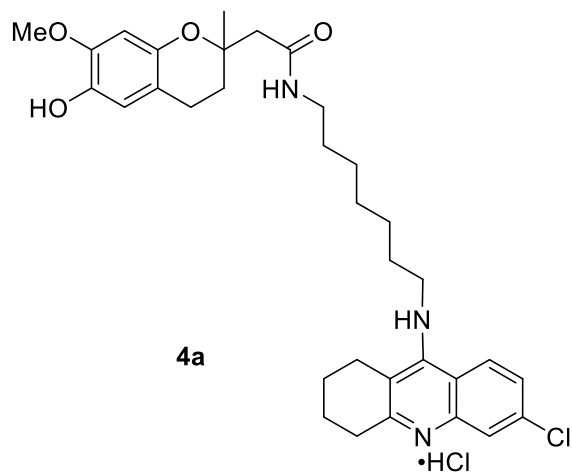
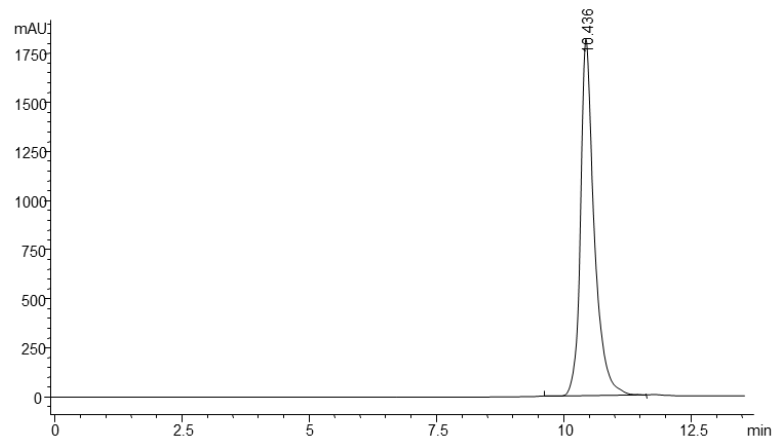
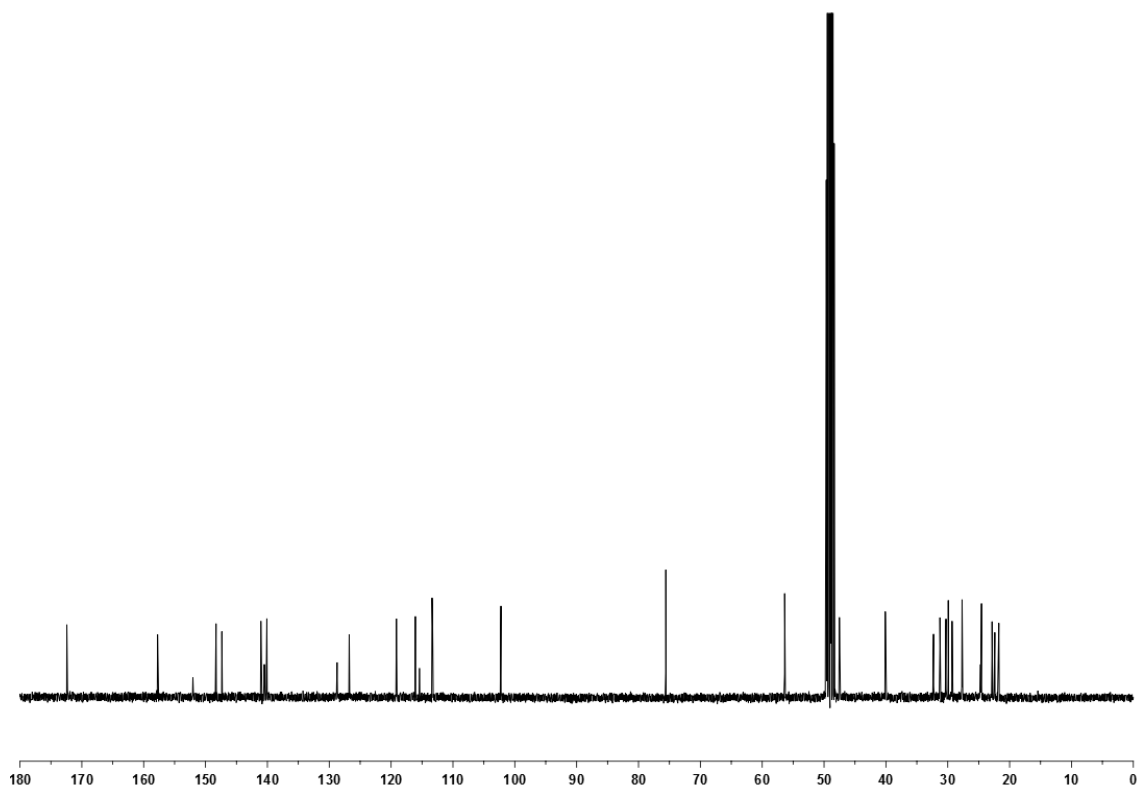


Figure S5. Representative snapshots of the complexes of (top) (*R*)-**6b** and (bottom) (*S*)-**6b** bound to hAChE, and the structurally related compounds **11b** and the *p*-benzoquinone metabolite of **4b**. For each complex selected residues relevant for interactions of the chlorotacrine unit at the catalytic site, and of the chroman scaffold (**6b**), the *O*-benzylated chroman scaffold (**11b**), and the ring-open *p*-benzoquinone (**4b** benzoquinone) at the peripheral site (characterized by Trp286) are highlighted. The panels on the right provide a representation of compounds **11b** and **4b** benzoquinone protruding from the gorge to the solvent, with the protein enclosed by the solvent-exposed surface.

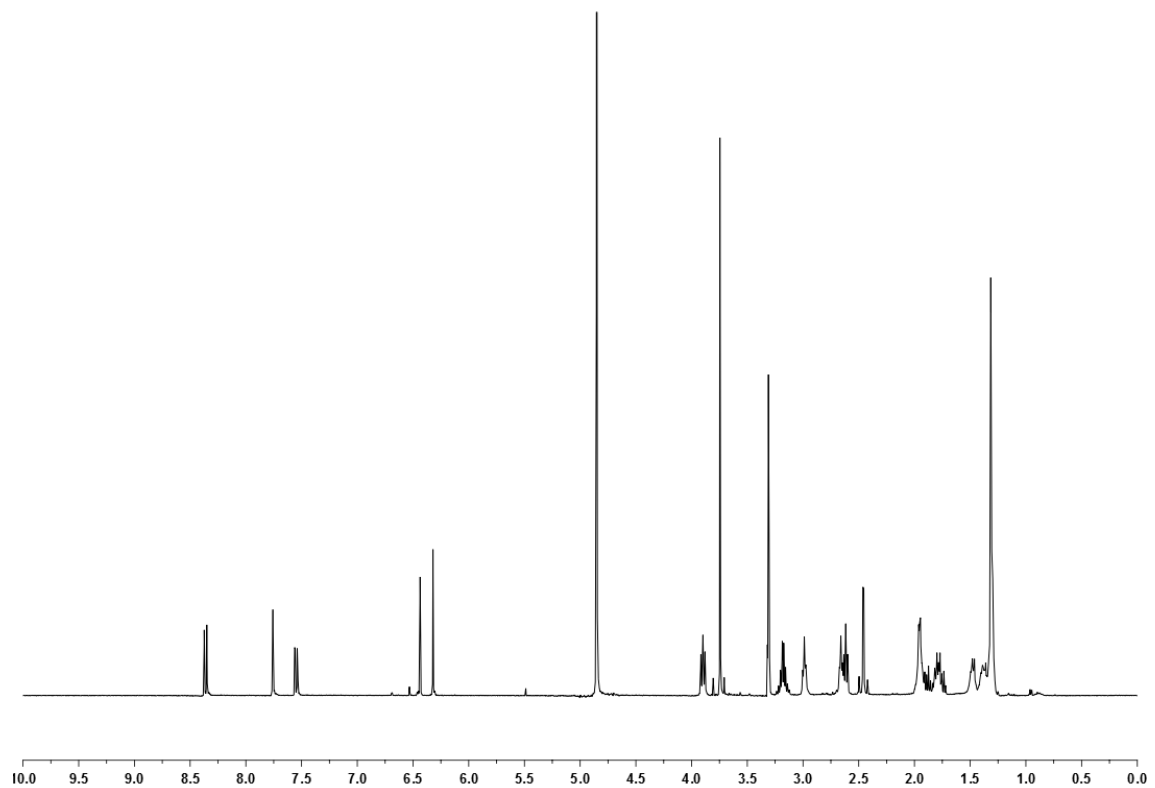
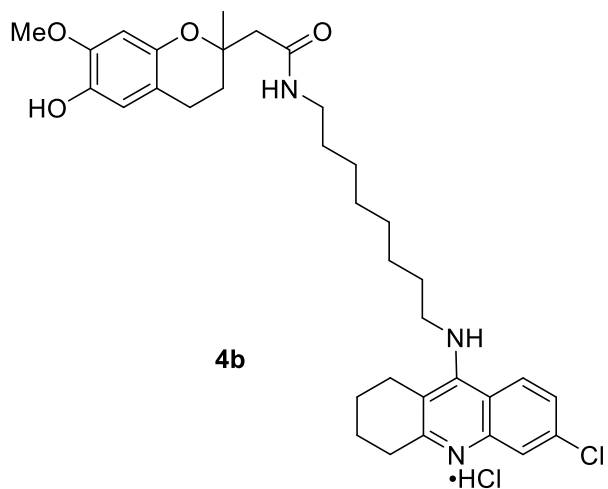
Copies of ^1H NMR (400 MHz, CD_3OD) and ^{13}C NMR (100.6 MHz, CD_3OD) spectra and HPLC chromatograms of target compounds

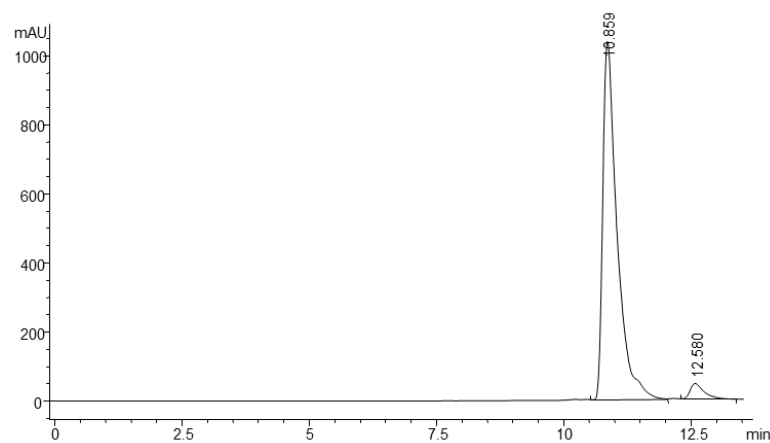
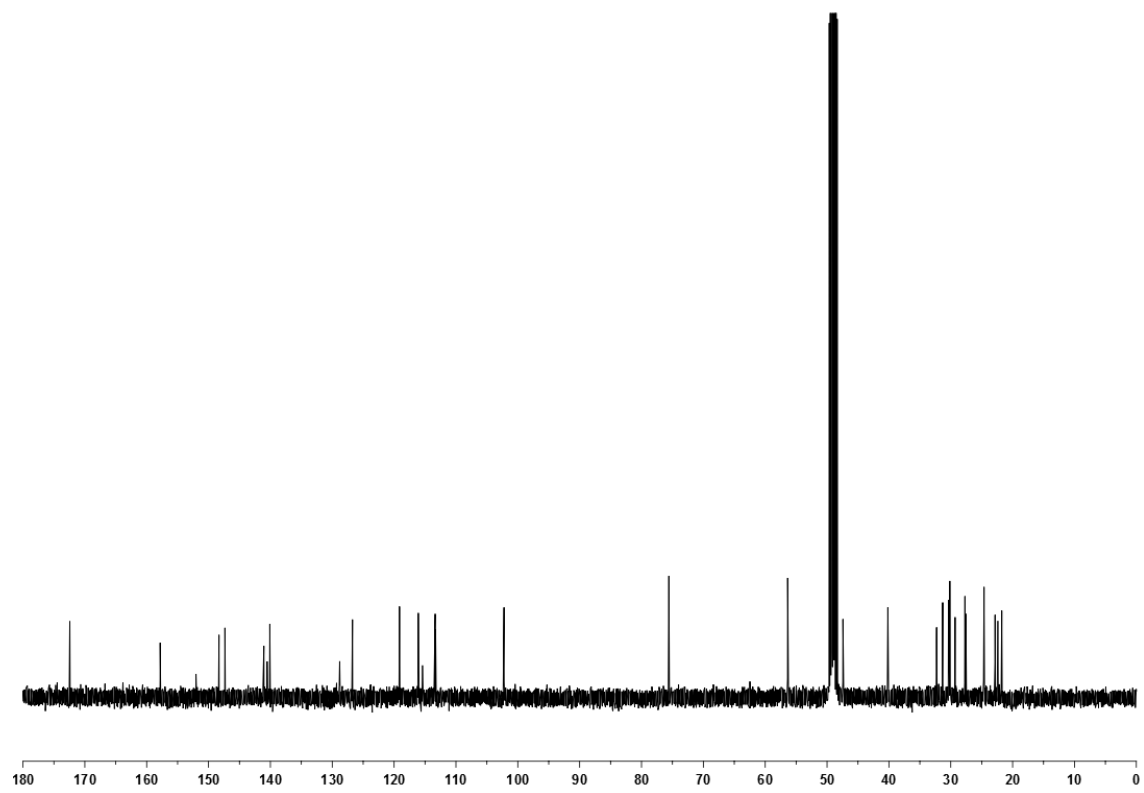
N-{7-[*(6-Chloro-1,2,3,4-tetrahydroacridin-9-yl)amino*]heptyl}-2-(6-hydroxy-7-methoxy-2-methylchroman-2-yl)acetamide (**4a**)



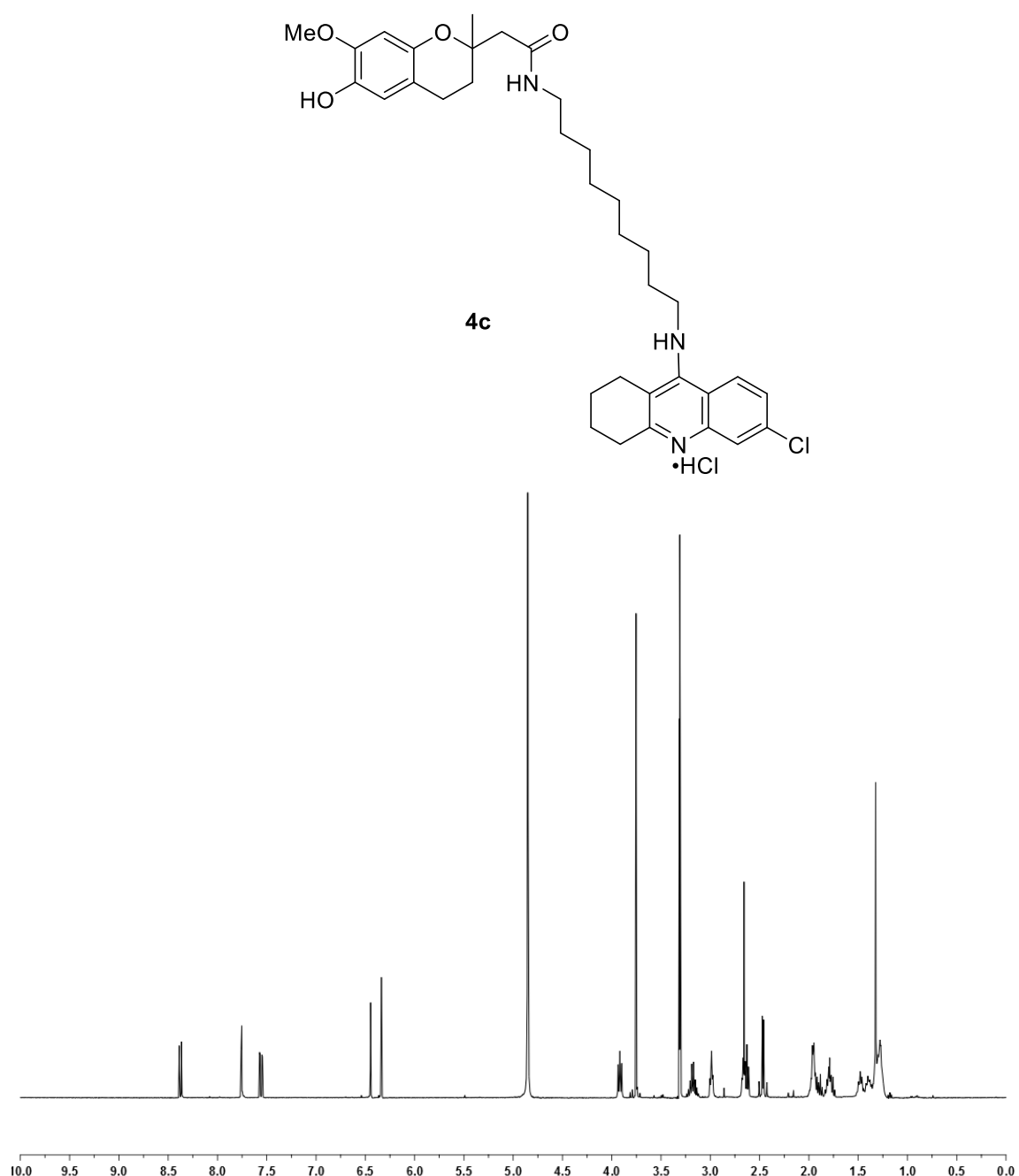


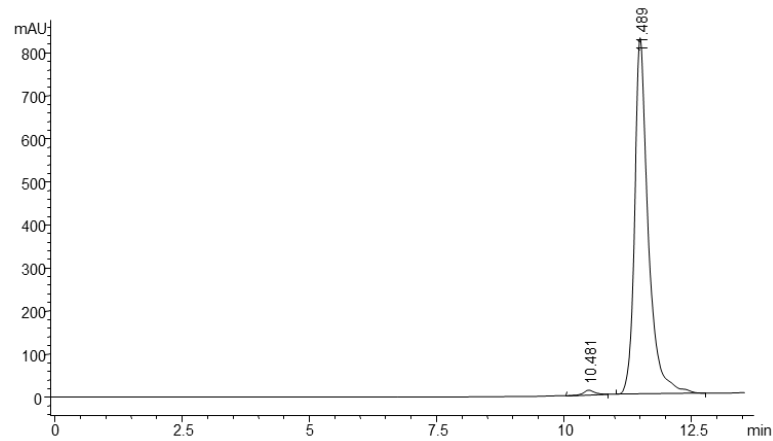
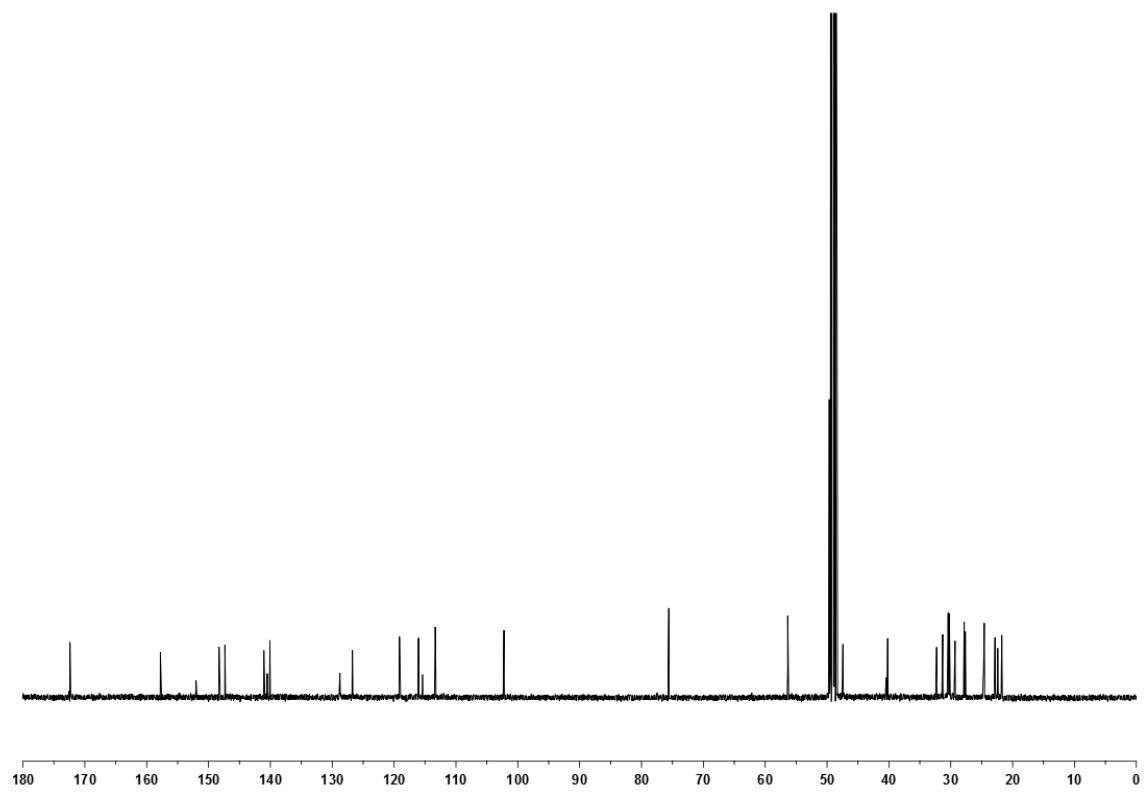
N-{8-[{(6-Chloro-1,2,3,4-tetrahydroacridin-9-yl)amino]octyl}-2-(6-hydroxy-7-methoxy-2-methylchroman-2-yl)acetamide (**4b**)



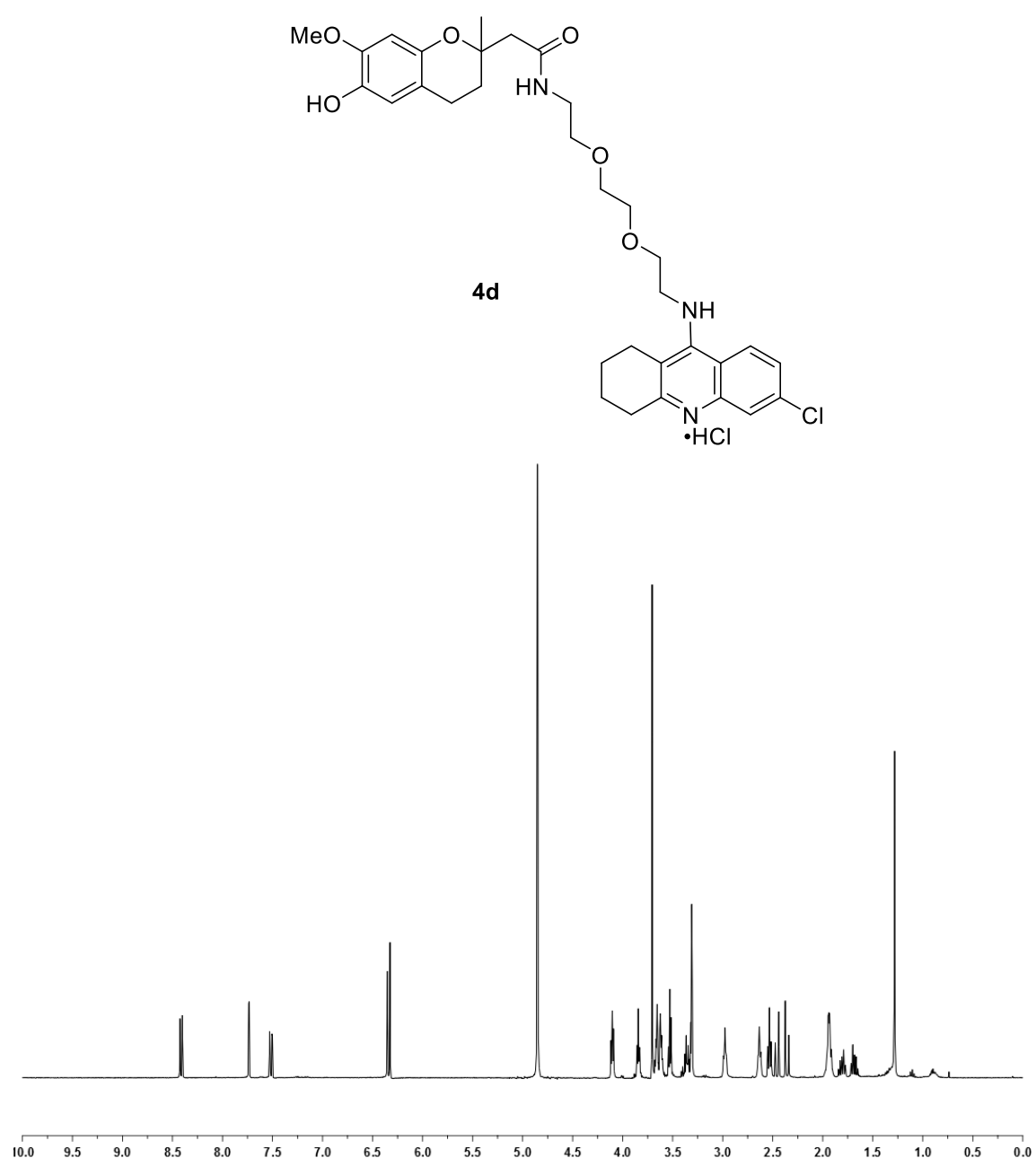


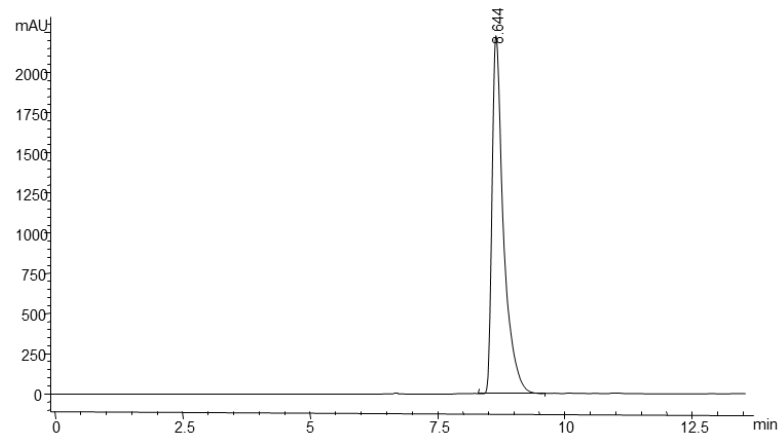
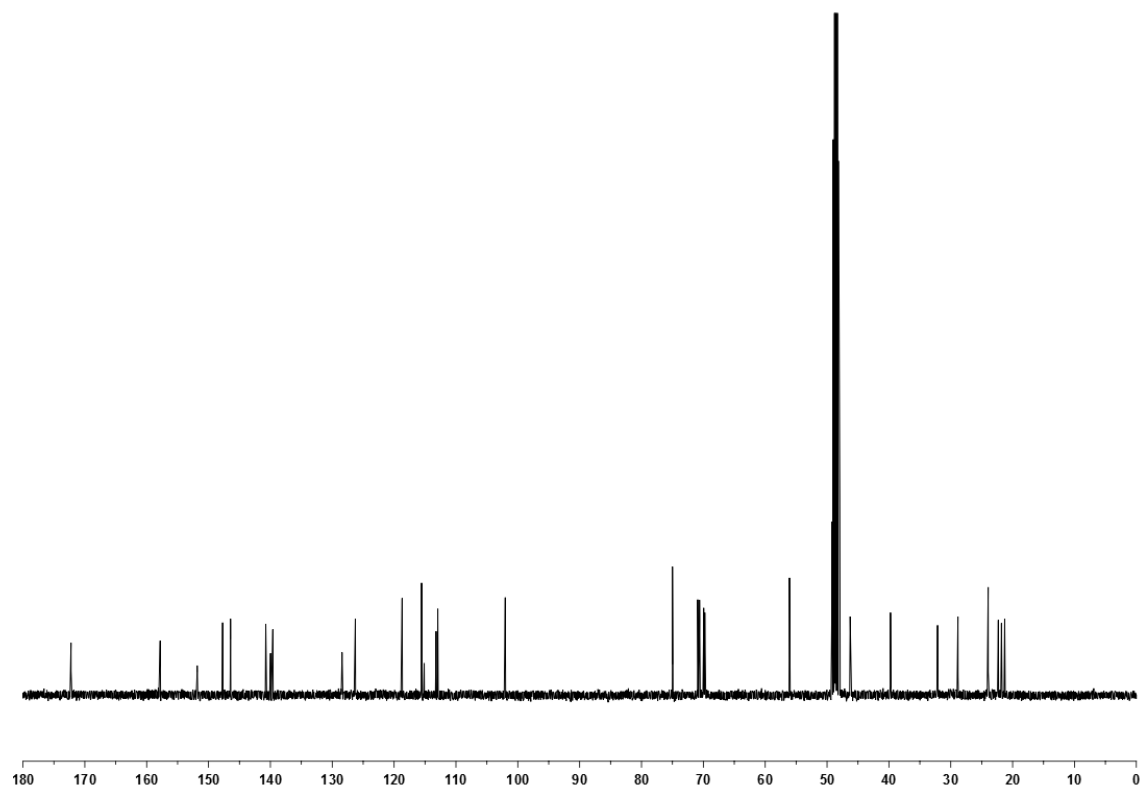
N-{9-[(6-Chloro-1,2,3,4-tetrahydroacridin-9-yl)amino]nonyl}-2-(6-hydroxy-7-methoxy-2-methylchroman-2-yl)acetamide (**4c**)



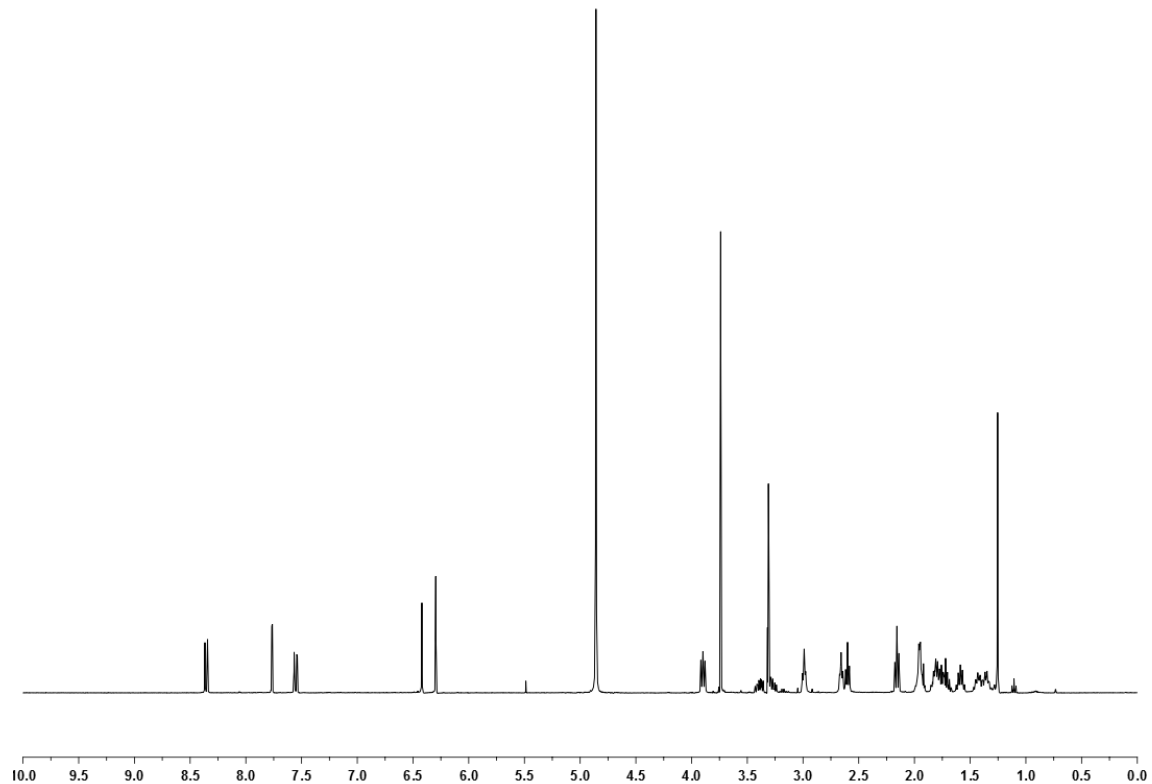
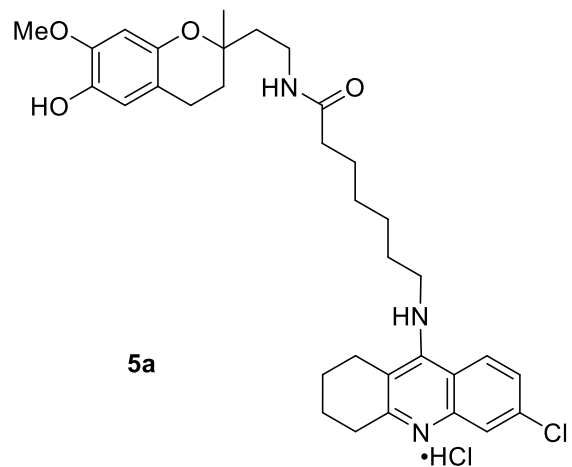


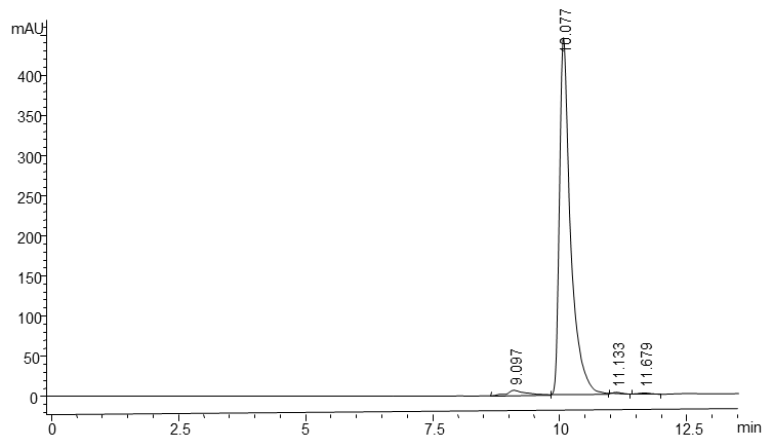
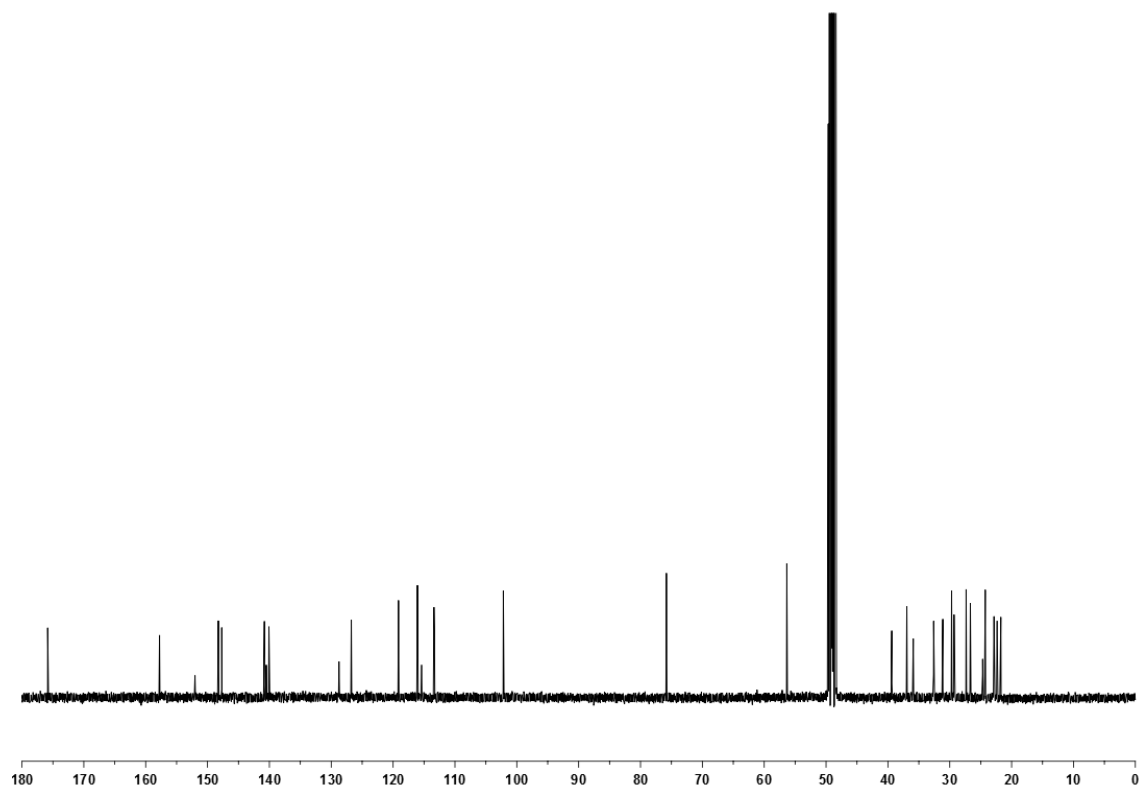
N-{8-[{(6-Chloro-1,2,3,4-tetrahydroacridin-9-yl)amino]-3,6-dioxaoctyl}-2-(6-hydroxy-7-methoxy-2-methylchroman-2-yl)acetamide (**4d**)



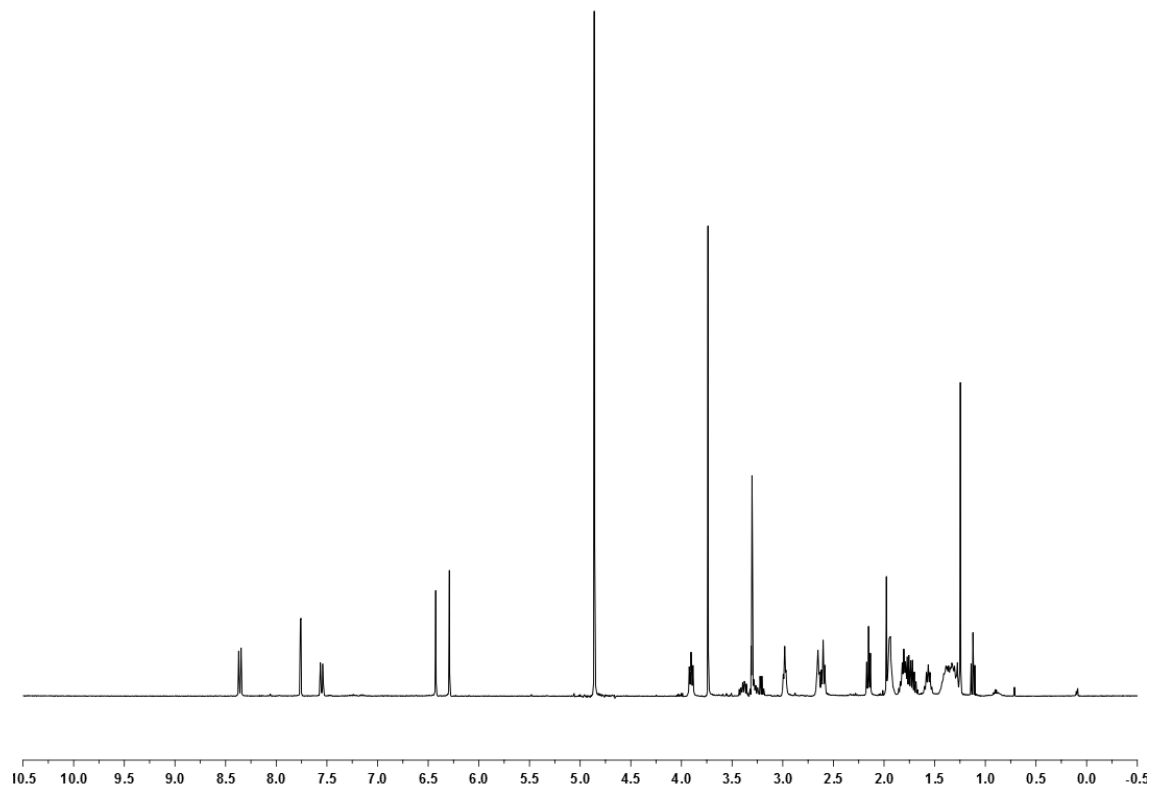
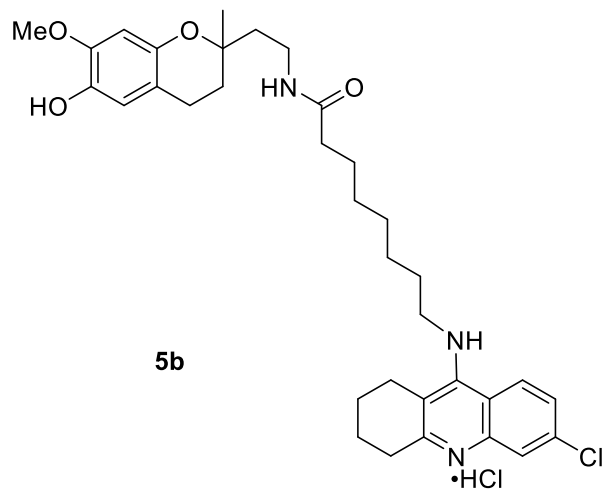


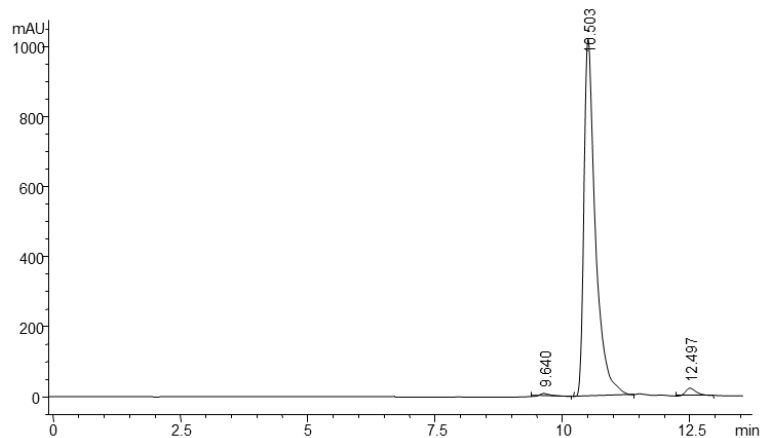
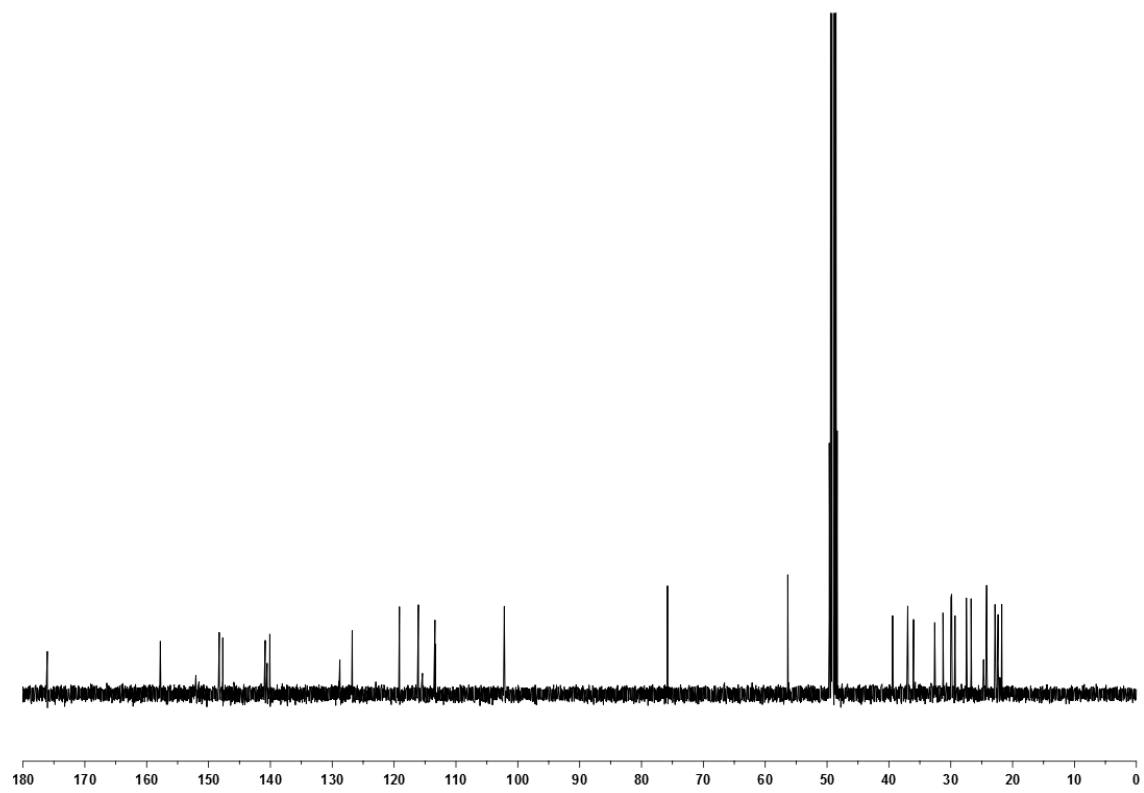
7-[(6-Chloro-1,2,3,4-tetrahydroacridin-9-yl)amino]-N-[2-(6-hydroxy-7-methoxy-2-methylchroman-2-yl)ethyl]heptanamide (**5a**)



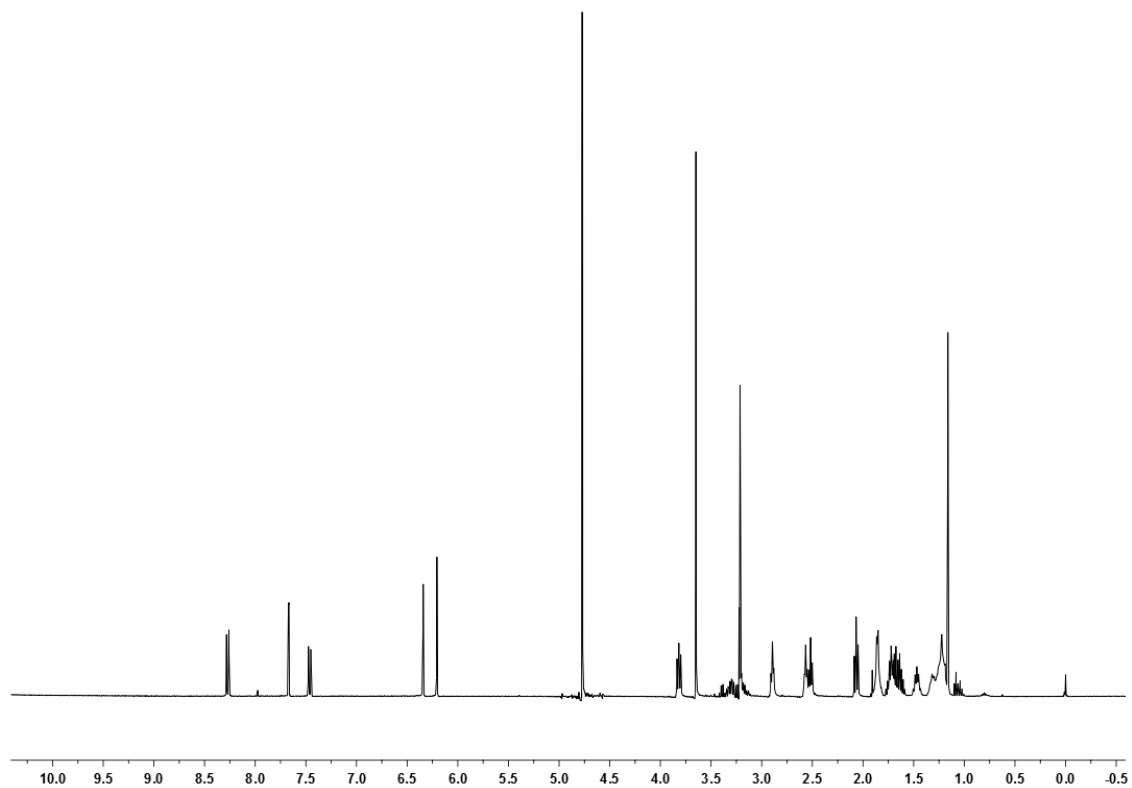
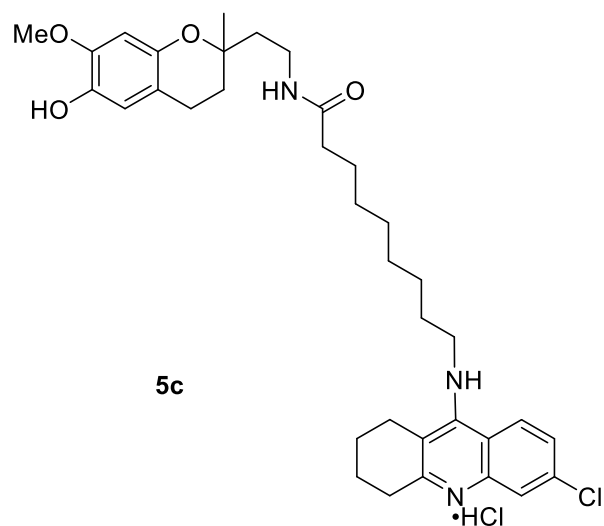


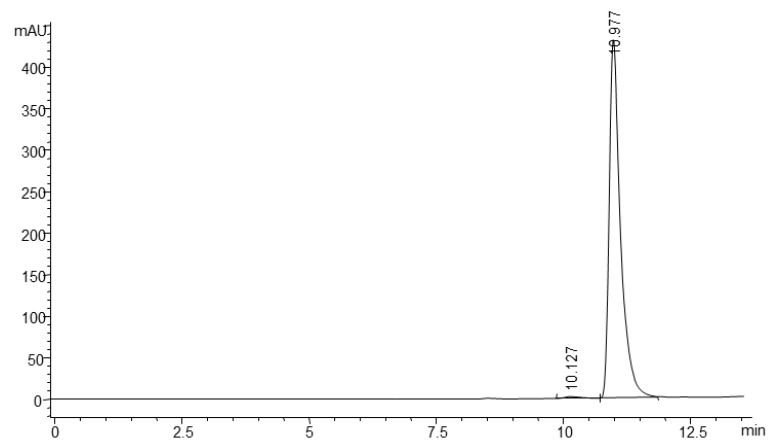
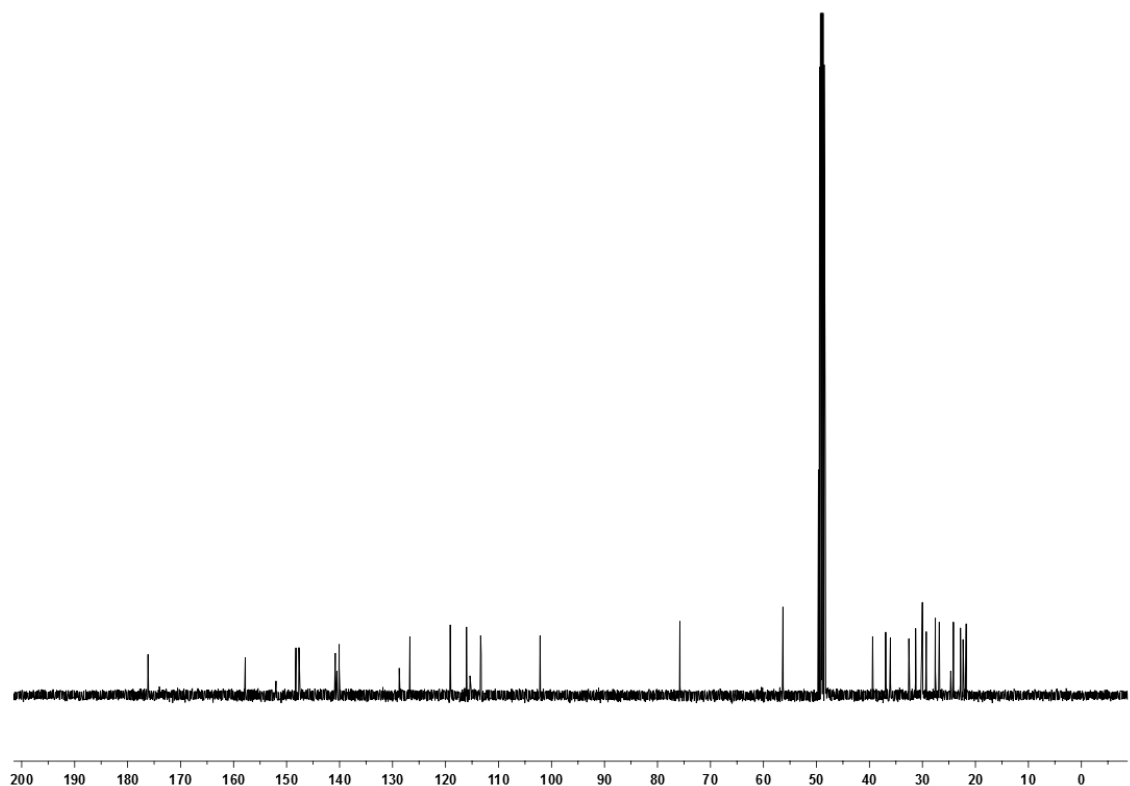
8-[(6-Chloro-1,2,3,4-tetrahydroacridin-9-yl)amino]-N-[2-(6-hydroxy-7-methoxy-2-methylchroman-2-yl)ethyl]octanamide (5b**)**



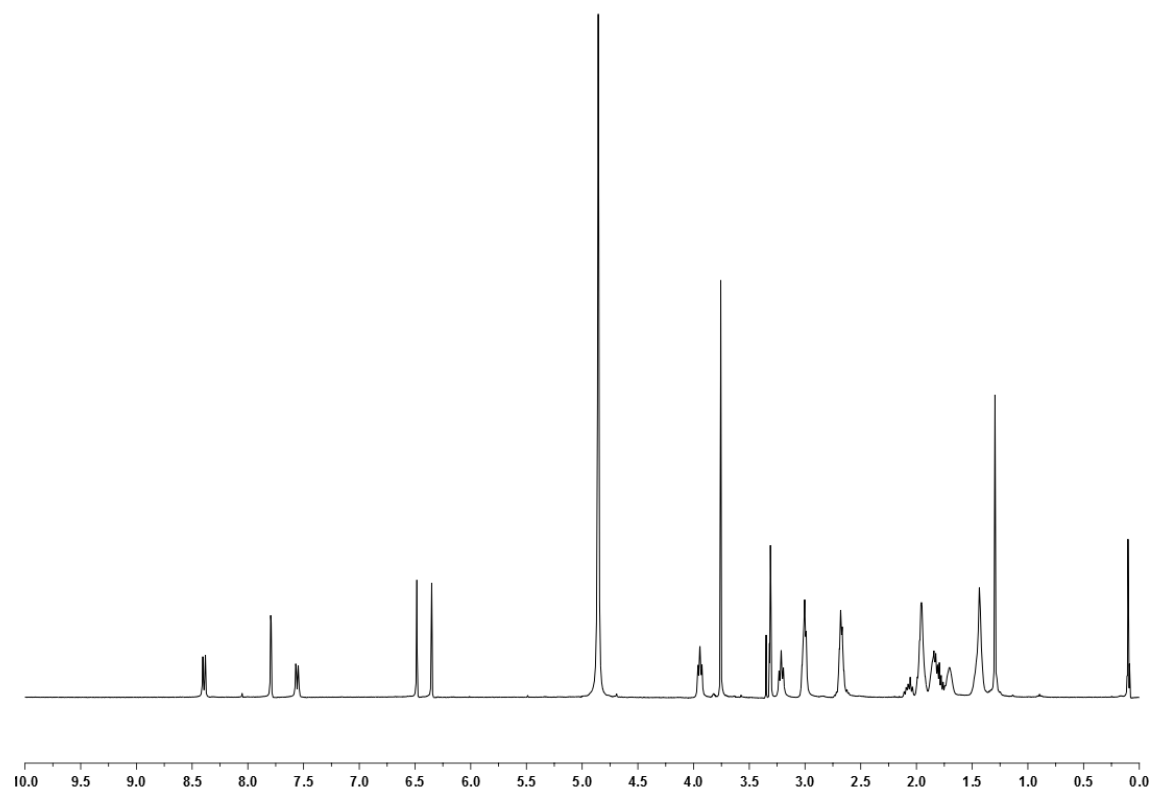
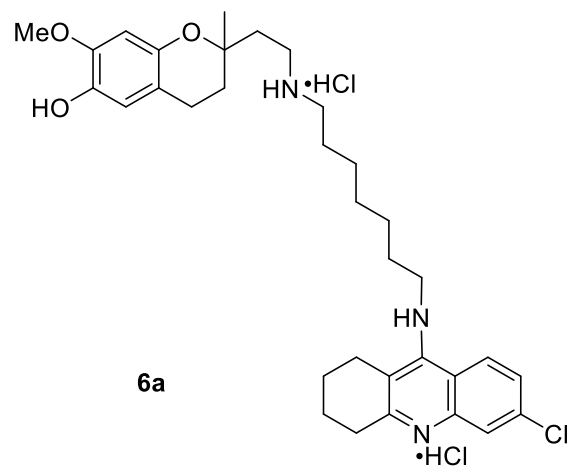


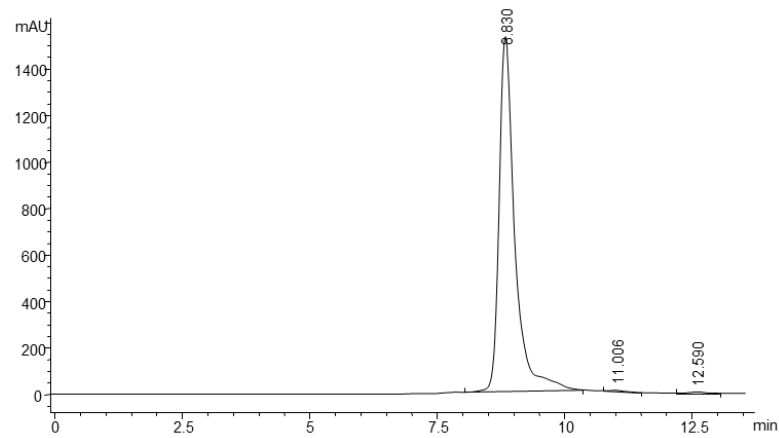
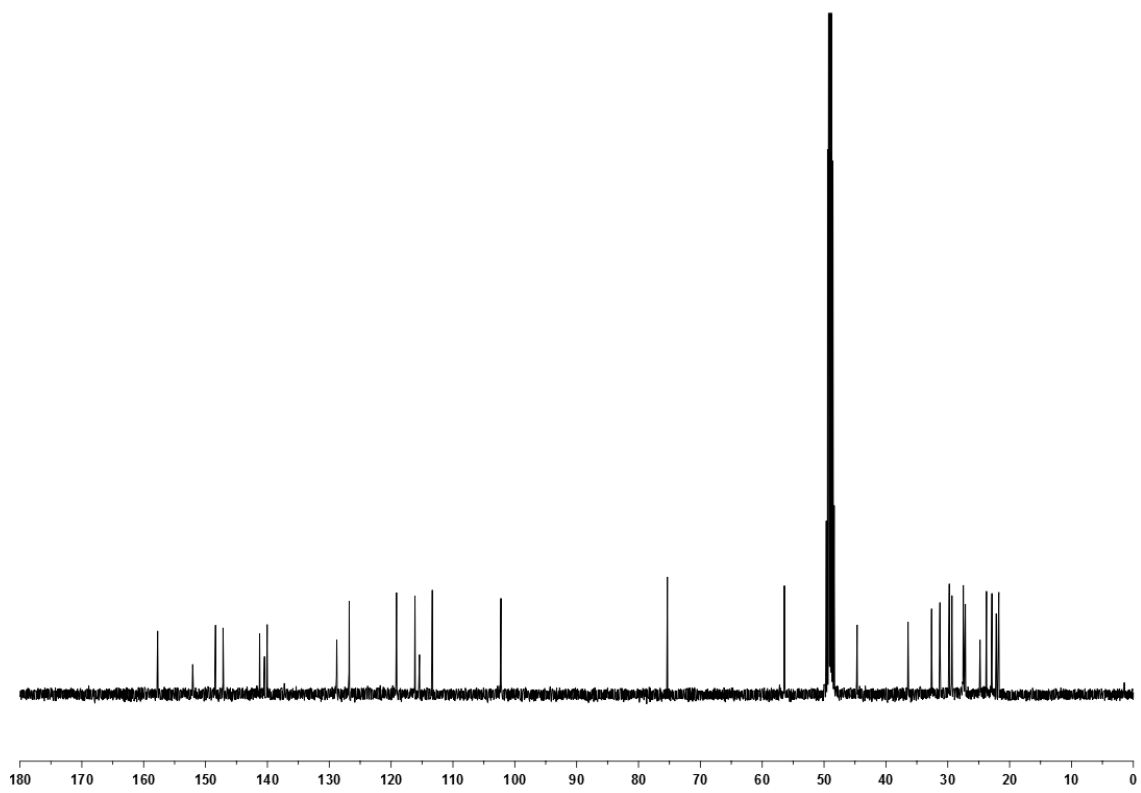
9-[(6-Chloro-1,2,3,4-tetrahydroacridin-9-yl)amino]-*N*-[2-(6-hydroxy-7-methoxy-2-methylchroman-2-yl)ethyl]nonanamide (**5c**)



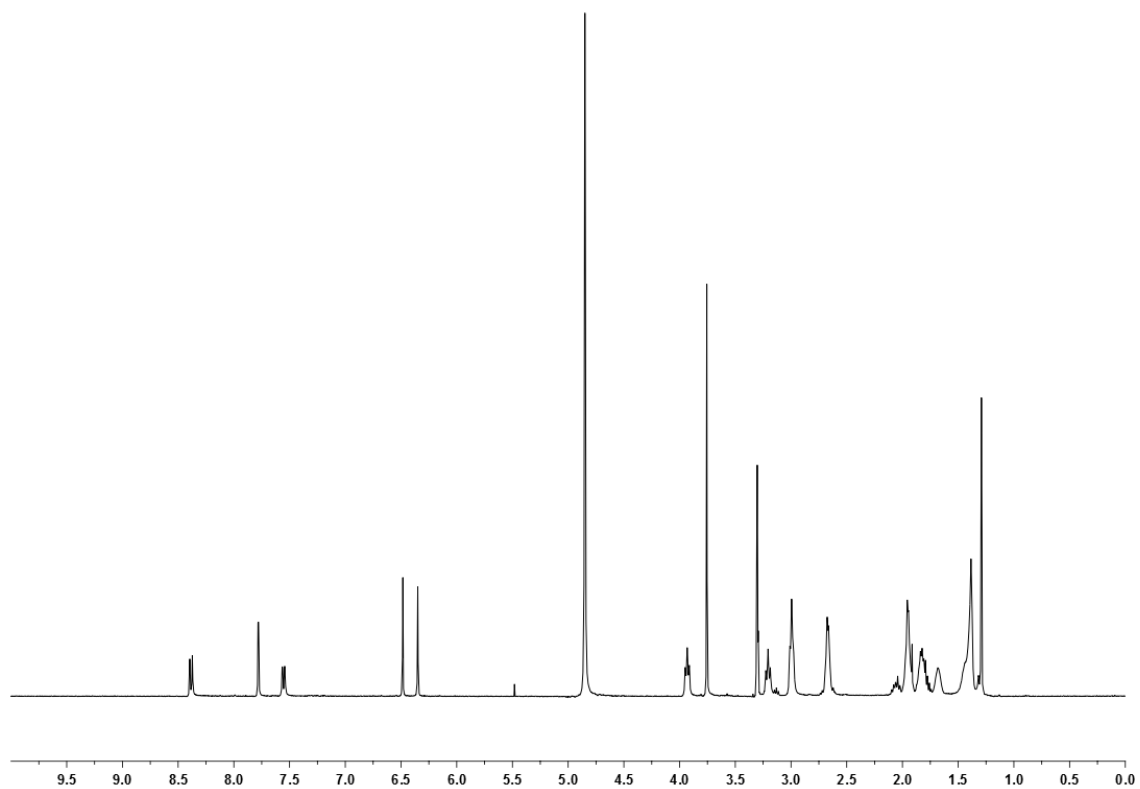
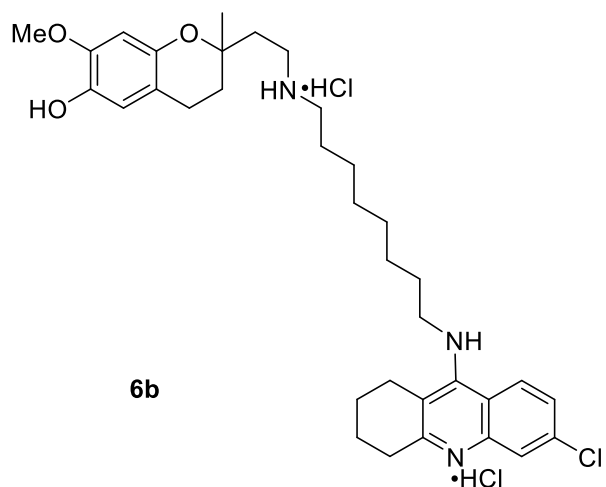


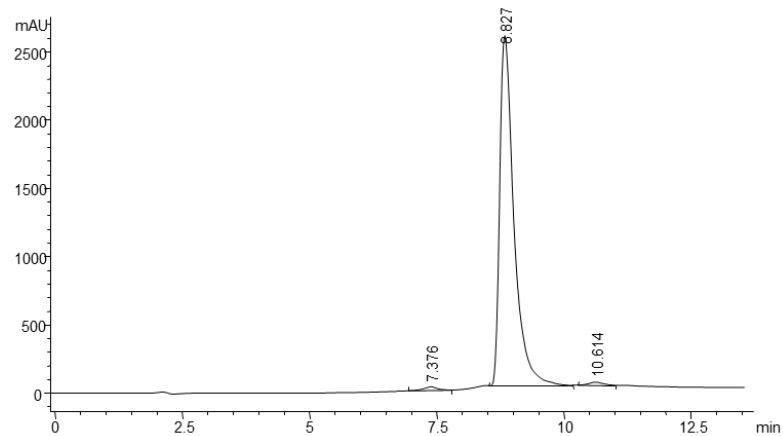
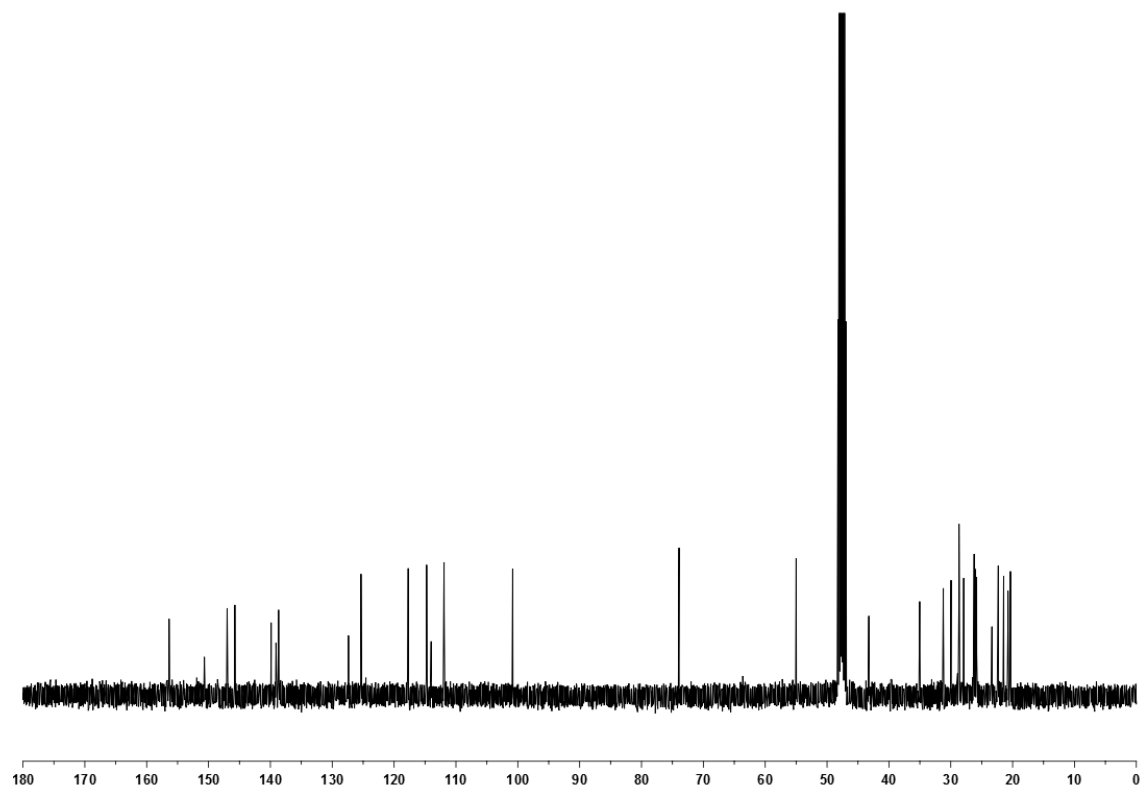
N-(6-Chloro-1,2,3,4-tetrahydroacridin-9-yl)-*N'*-[2-(6-hydroxy-7-methoxy-2-methylchroman-2-yl)ethyl]heptane-1,7-diamine (**6a**)



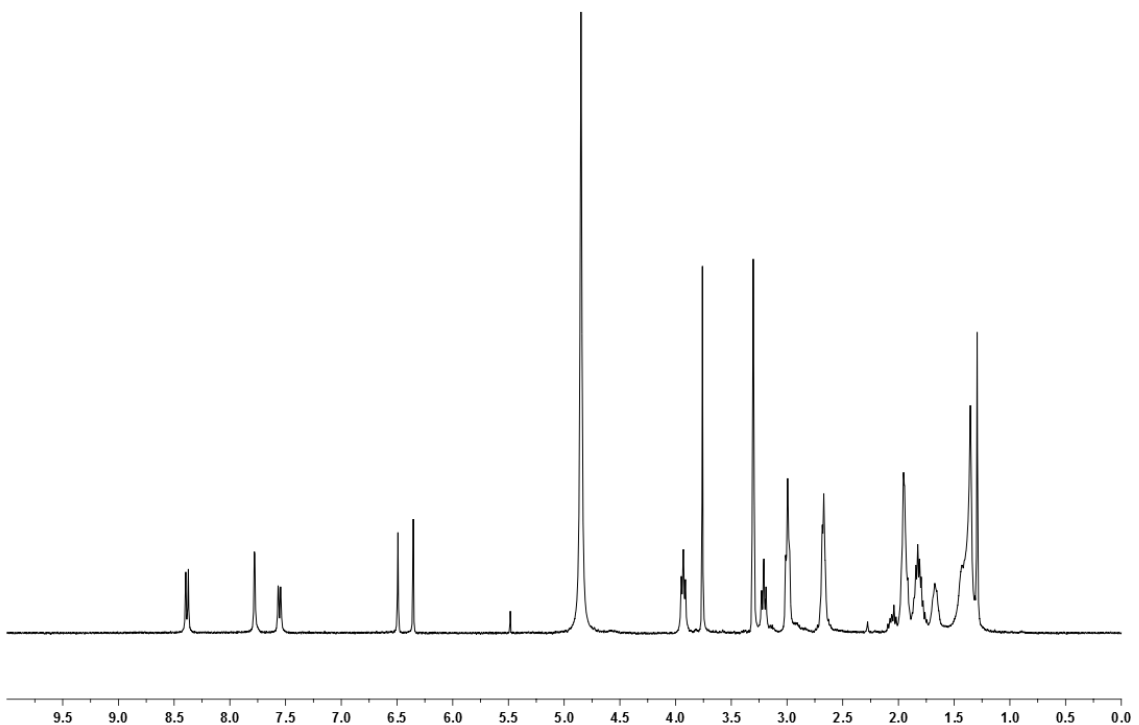
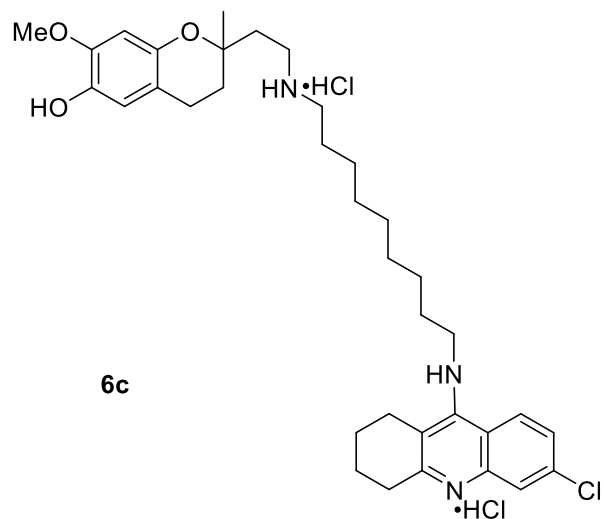


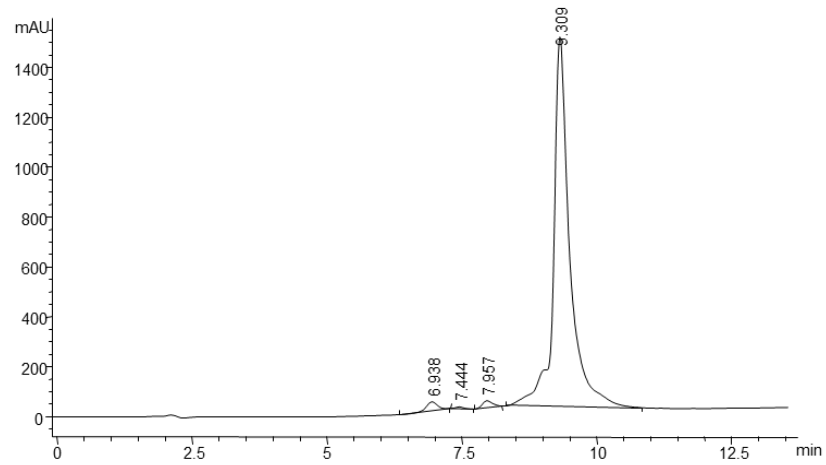
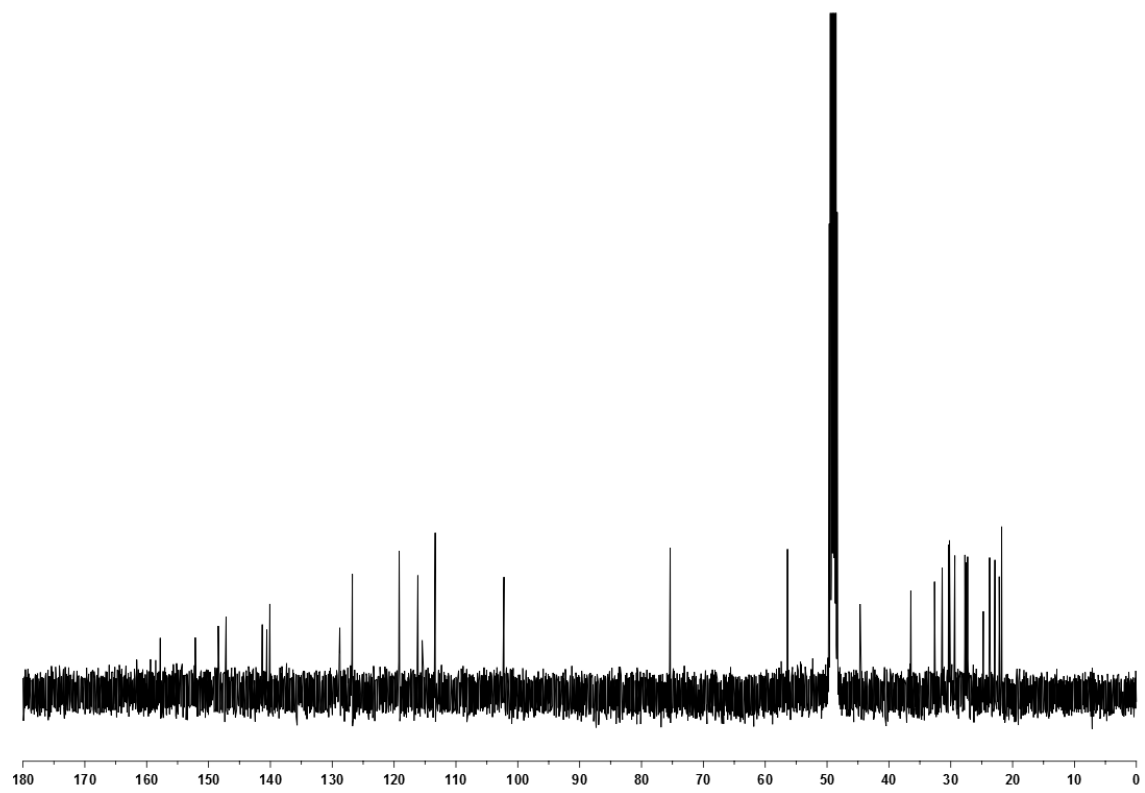
N-(6-Chloro-1,2,3,4-tetrahydroacridin-9-yl)-*N'*-[2-(6-hydroxy-7-methoxy-2-methylchroman-2-yl)ethyl]octane-1,8-diamine (**6b**)



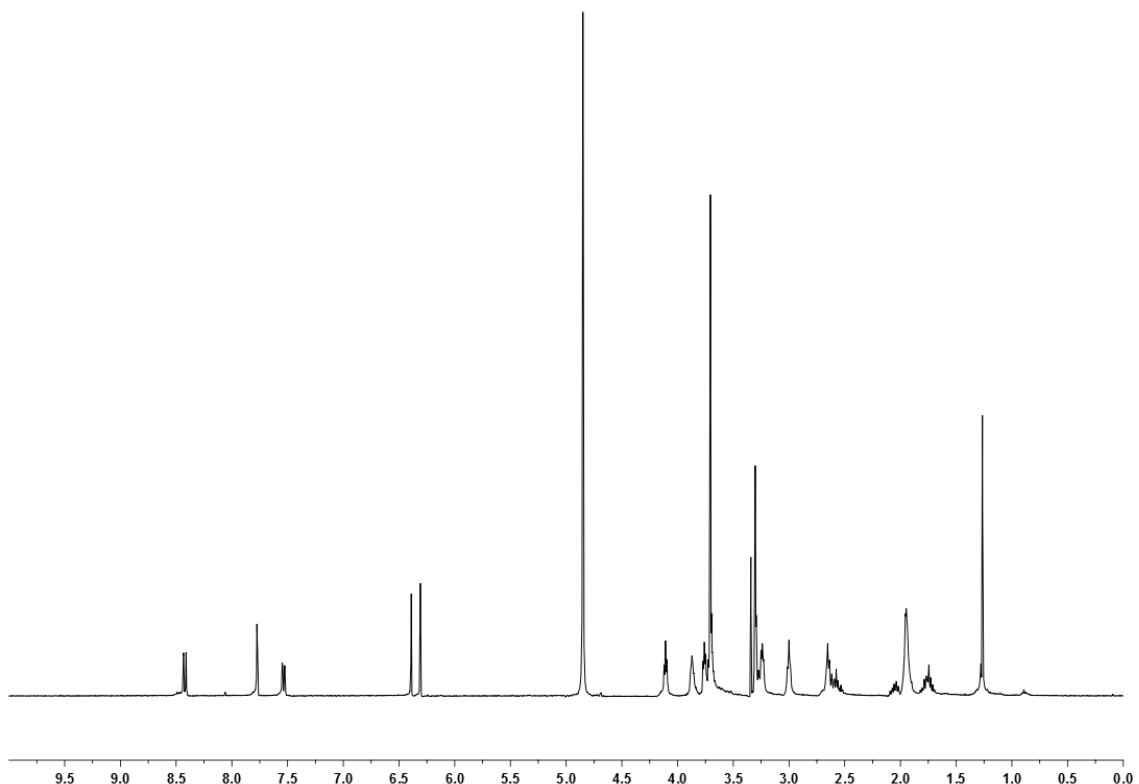
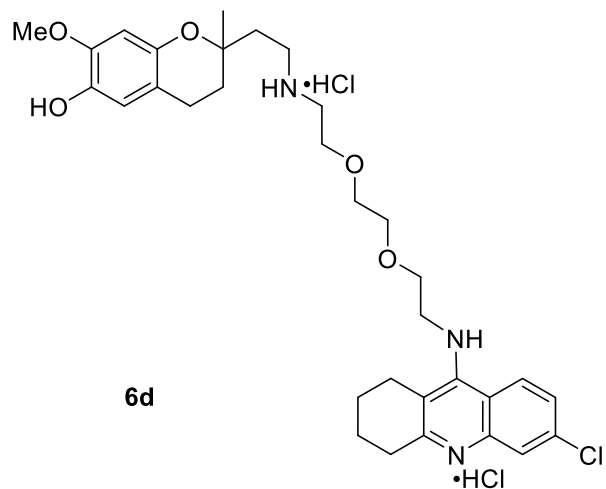


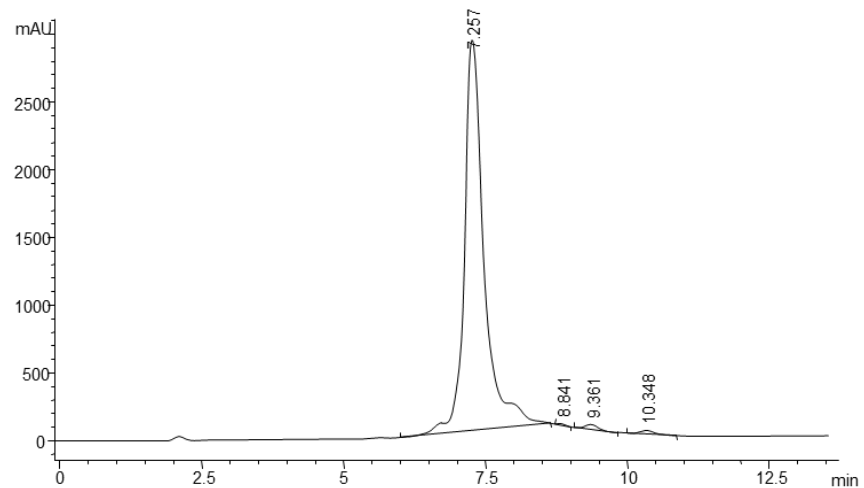
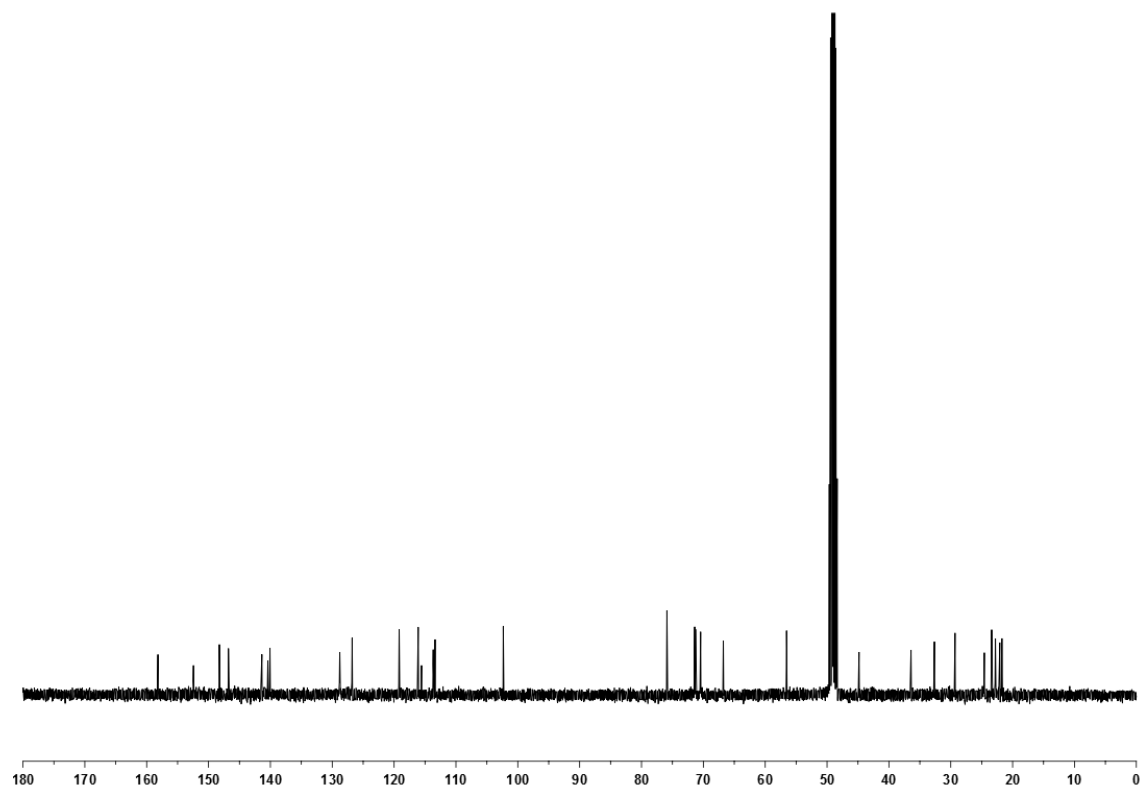
N-(6-Chloro-1,2,3,4-tetrahydroacridin-9-yl)-*N'*-[2-(6-hydroxy-7-methoxy-2-methylchroman-2-yl)ethyl]nonane-1,9-diamine (**6c**)



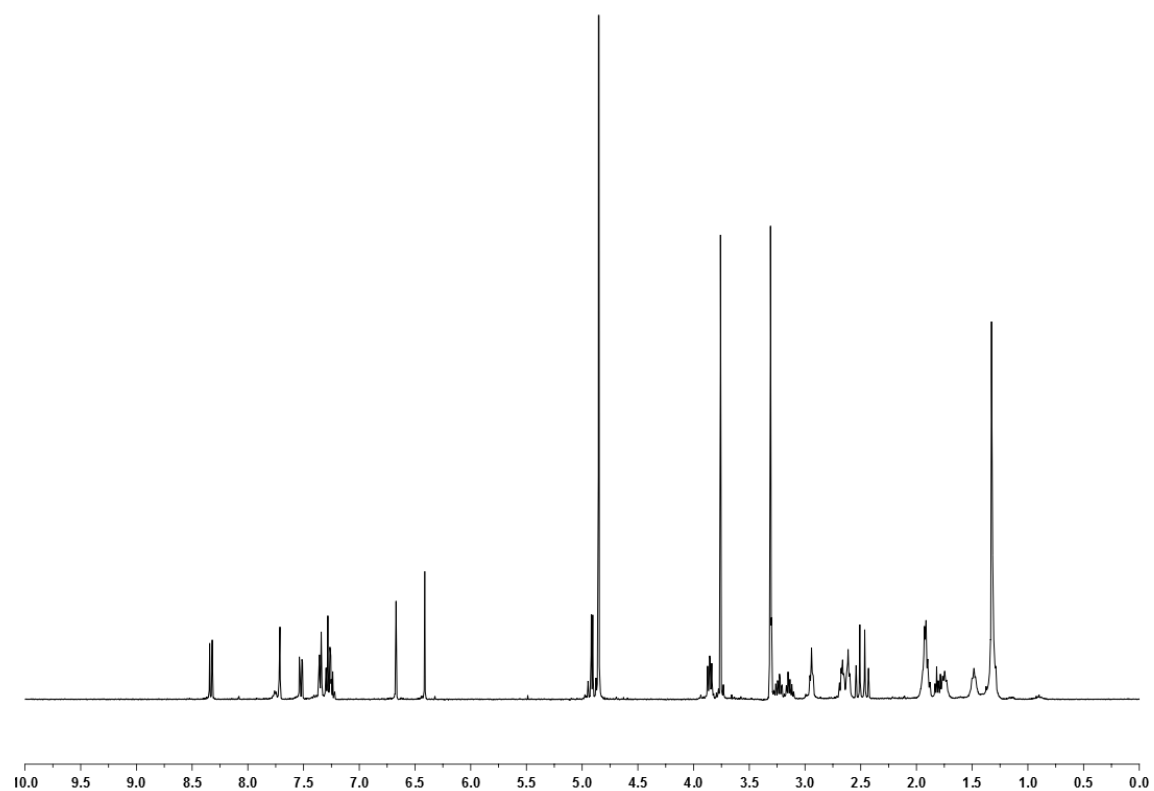
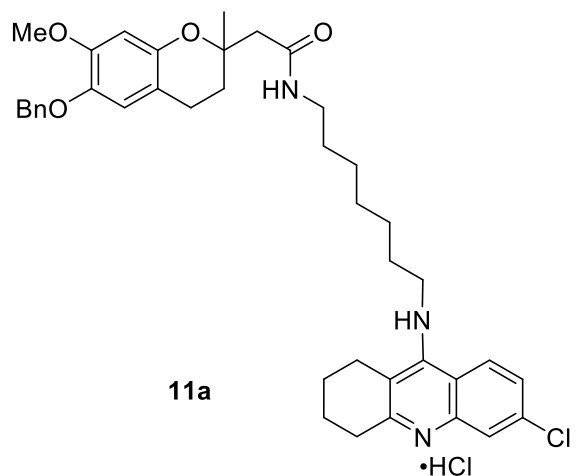


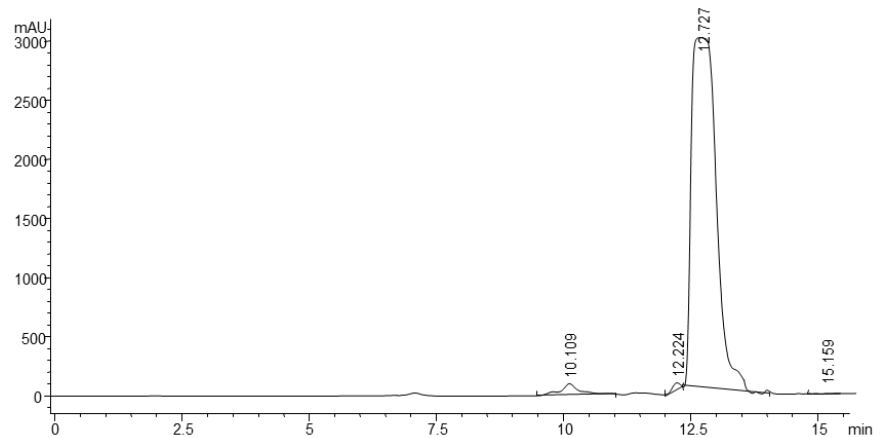
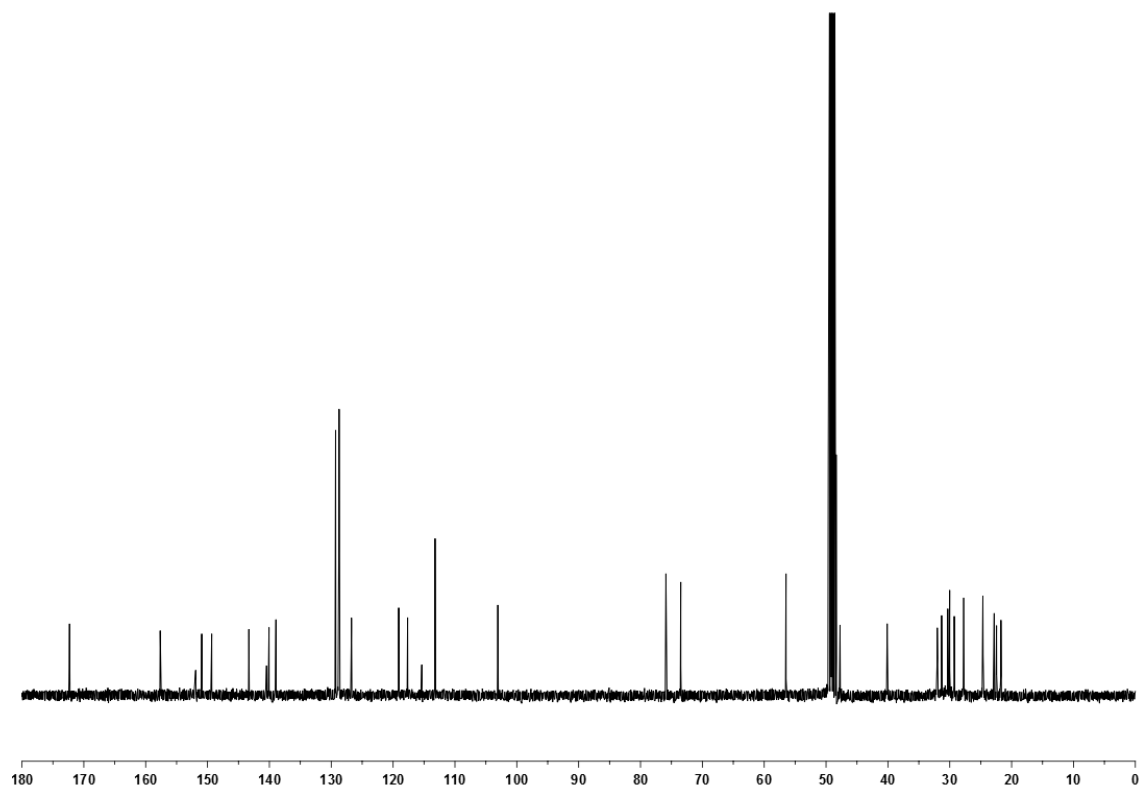
N-(6-Chloro-1,2,3,4-tetrahydroacridin-9-yl)-*N'*-[2-(6-hydroxy-7-methoxy-2-methylchroman-2-yl)ethyl]-3,6-dioxaoctane-1,8-diamine (**6d**)



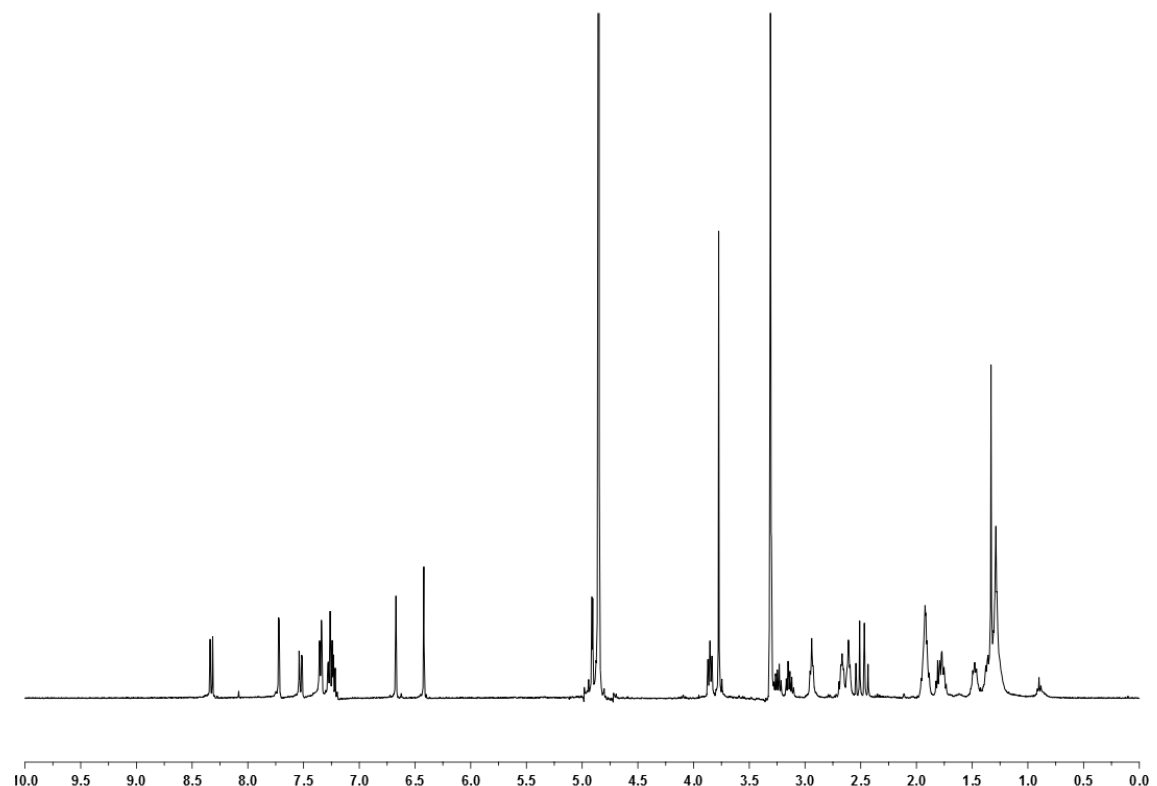
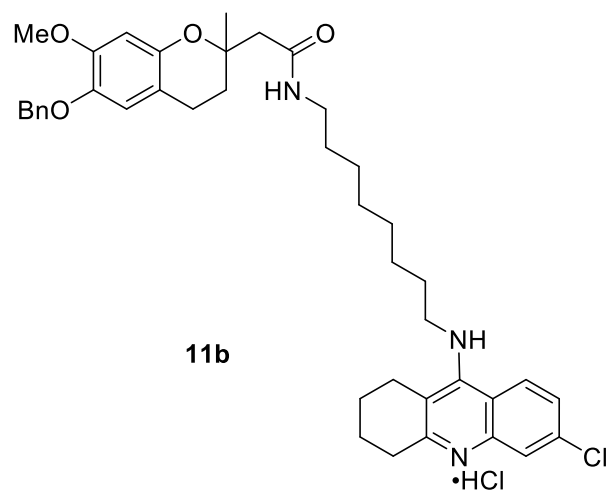


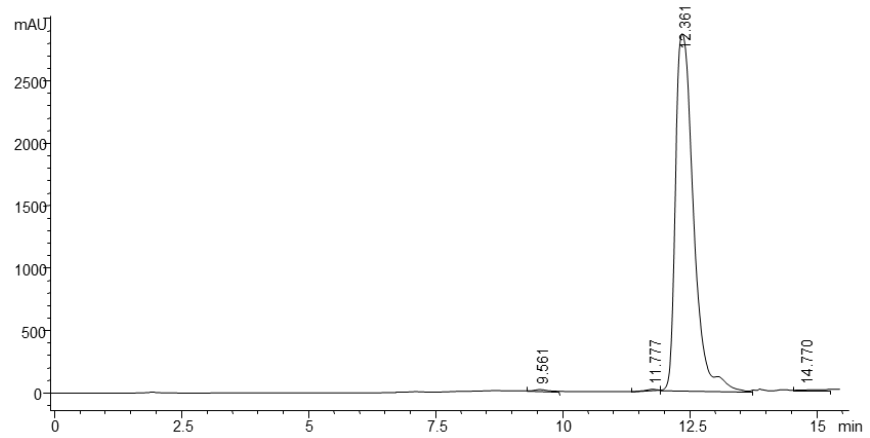
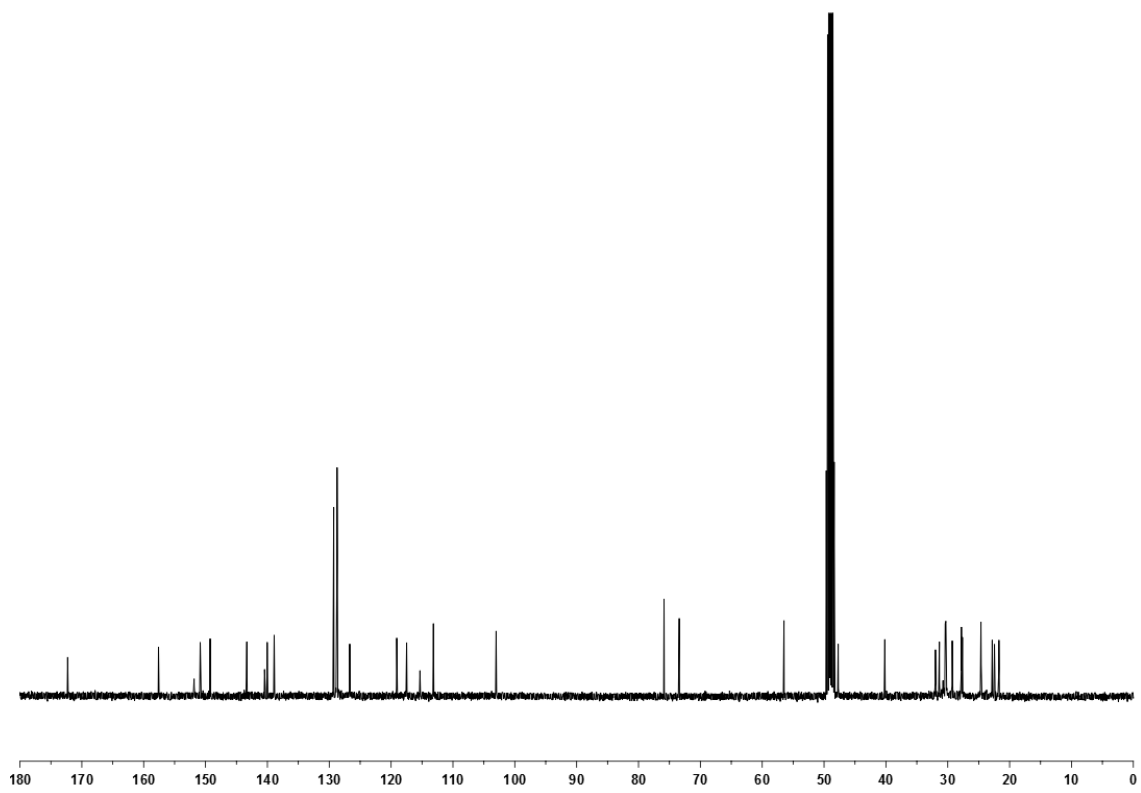
N-{7-[{(6-Chloro-1,2,3,4-tetrahydroacridin-9-yl)amino]heptyl}-2-(6-benzyloxy-7-methoxy-2-methylchroman-2-yl)acetamide (**11a**)



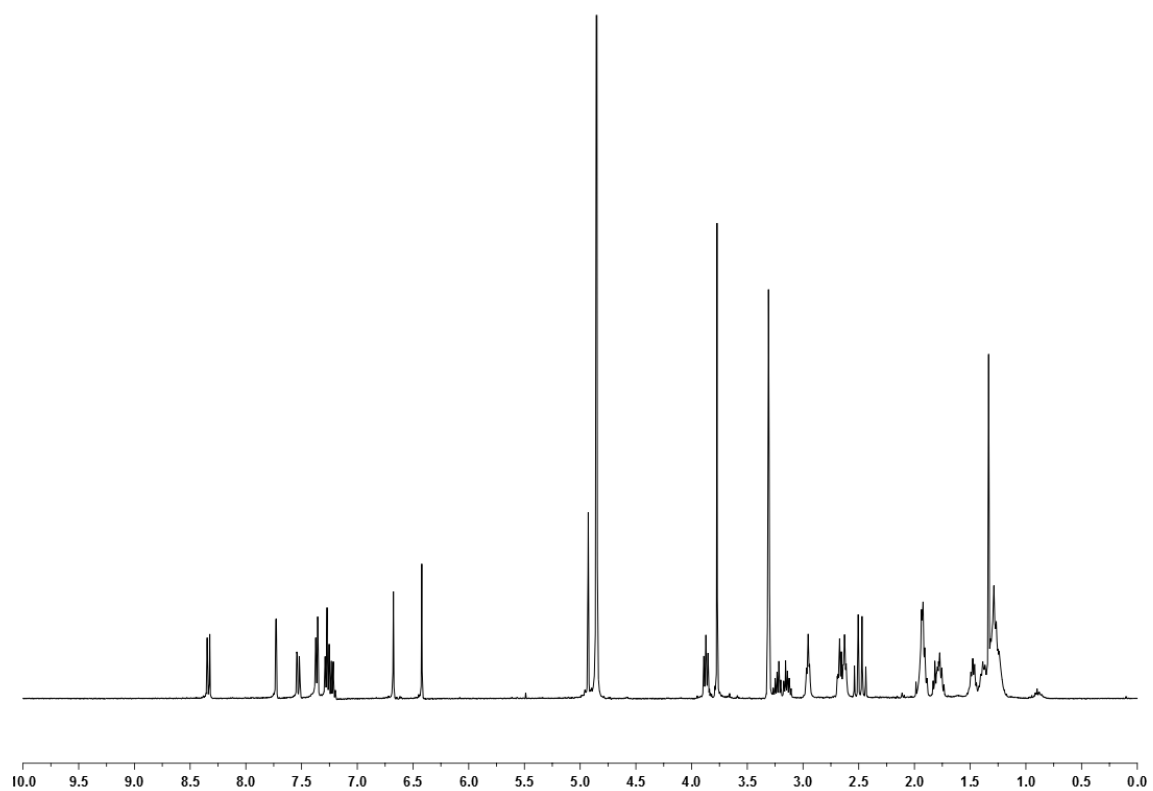
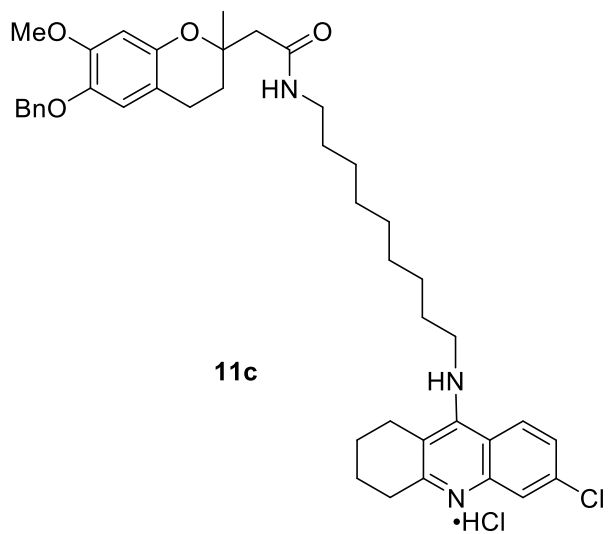


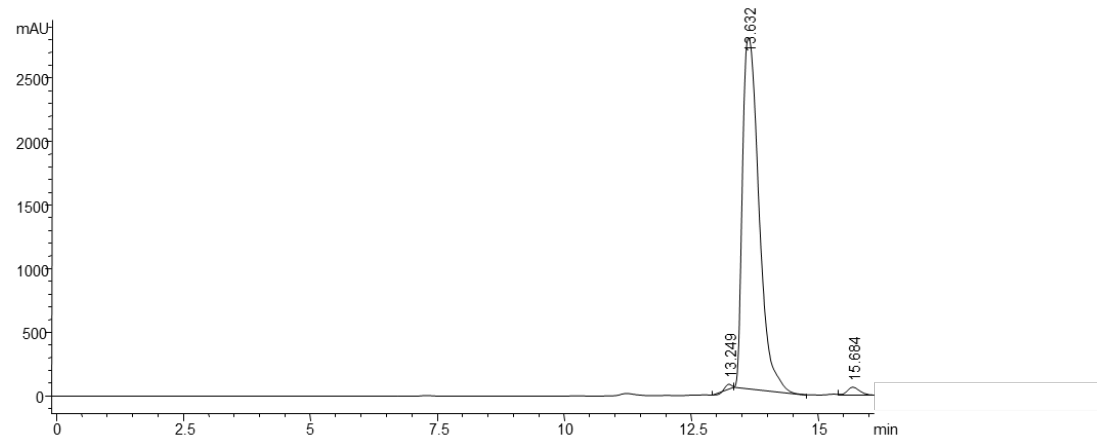
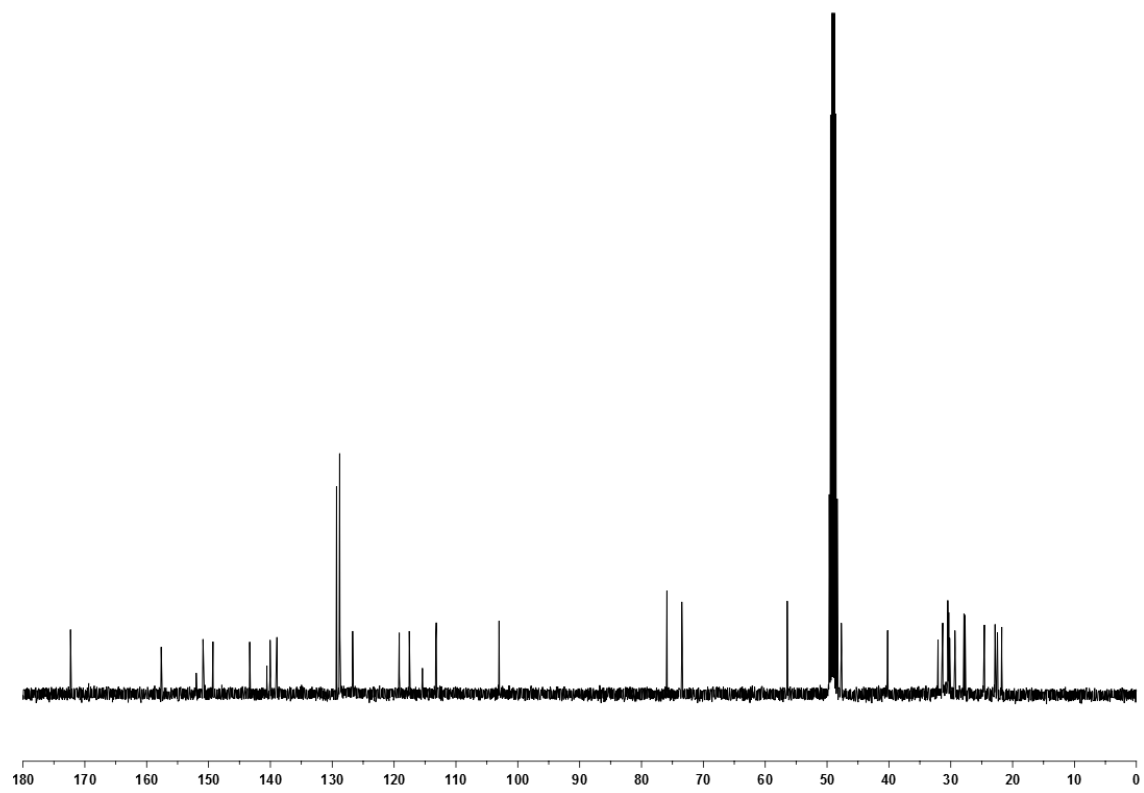
N-{8-[*(6-Chloro-1,2,3,4-tetrahydroacridin-9-yl)amino*]octyl}-2-(6-benzyloxy-7-methoxy-2-methylchroman-2-yl)acetamide (**11b**)



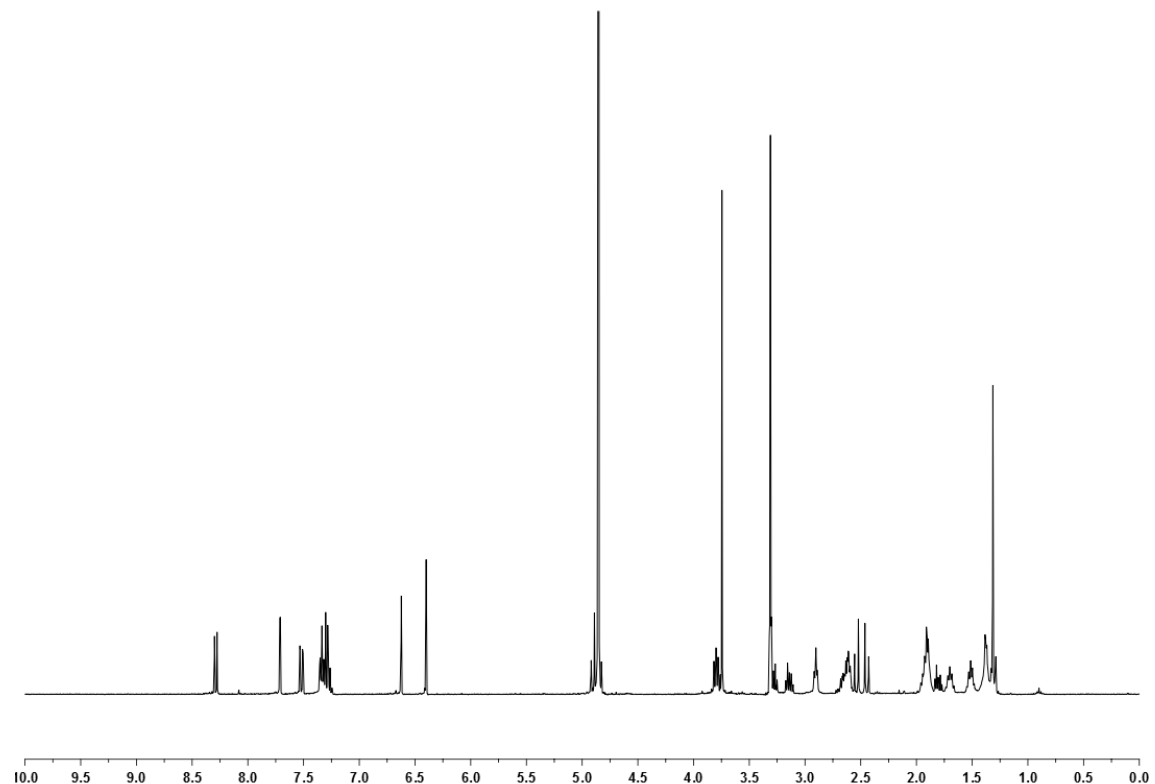
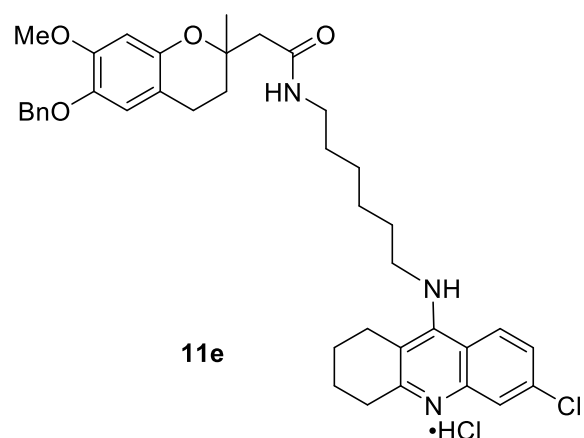


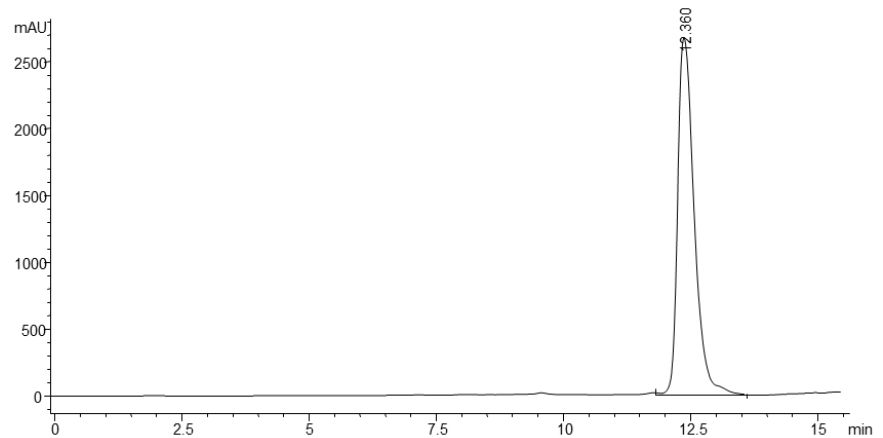
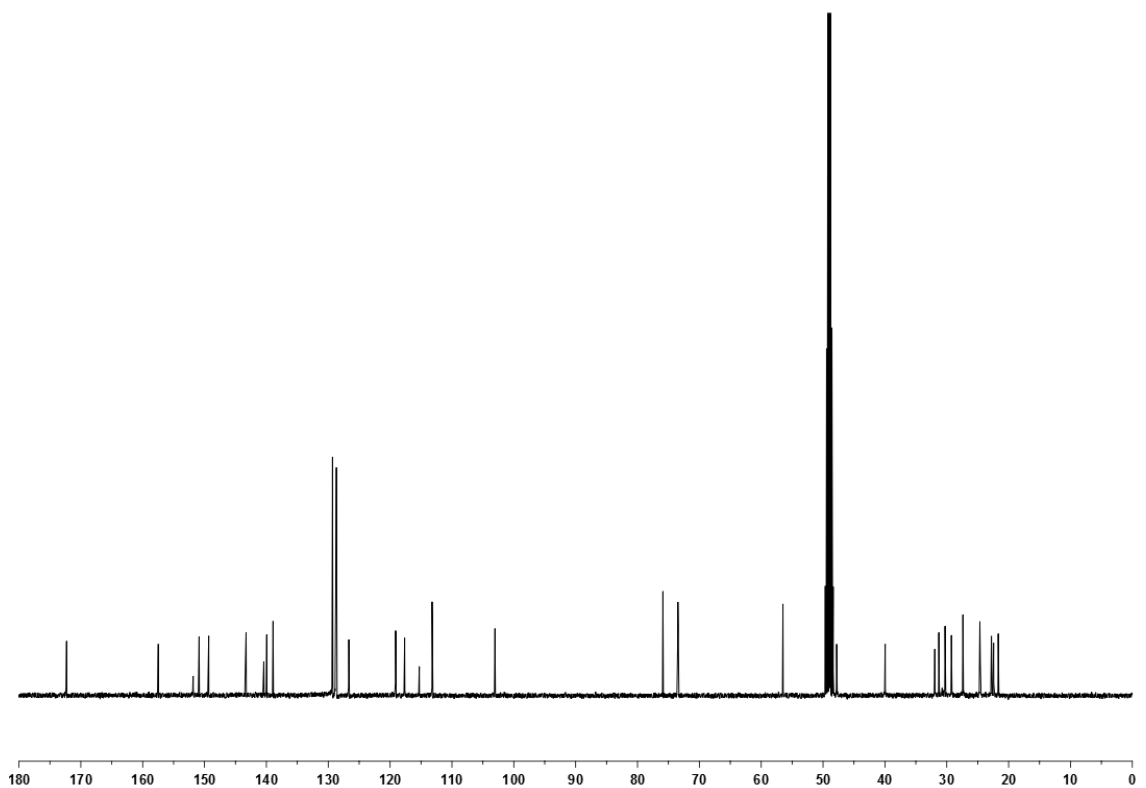
N-{9-[(6-Chloro-1,2,3,4-tetrahydroacridin-9-yl)amino]nonyl}-2-(6-benzyloxy-7-methoxy-2-methylchroman-2-yl)acetamide (**11c**)



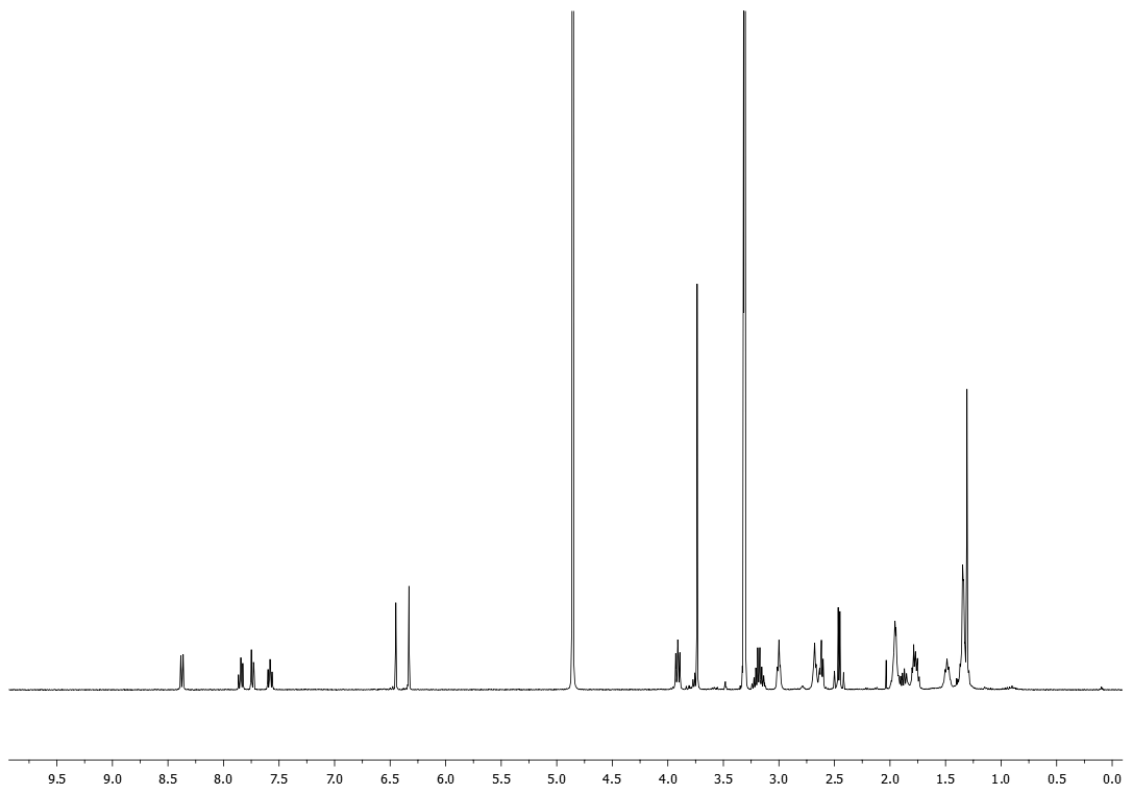
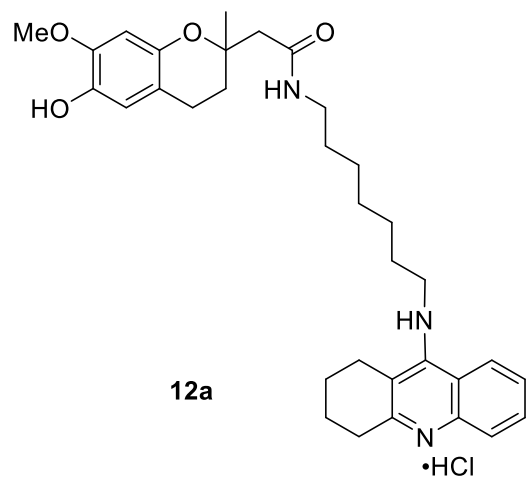


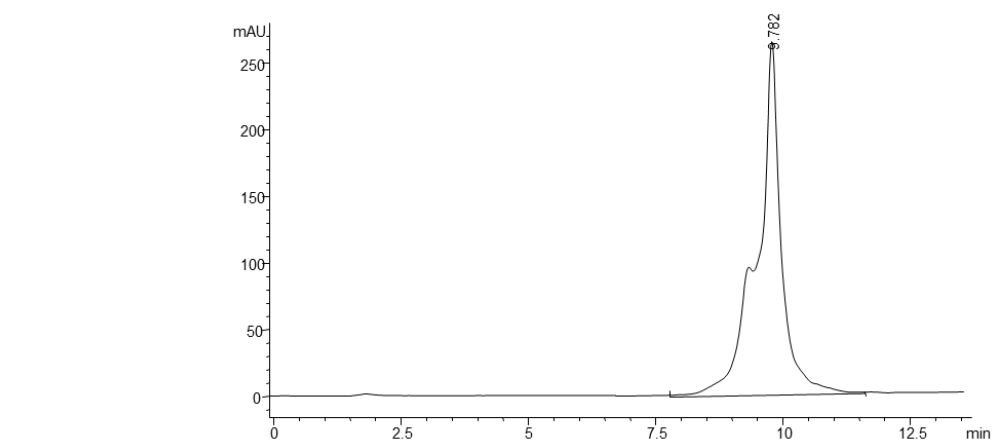
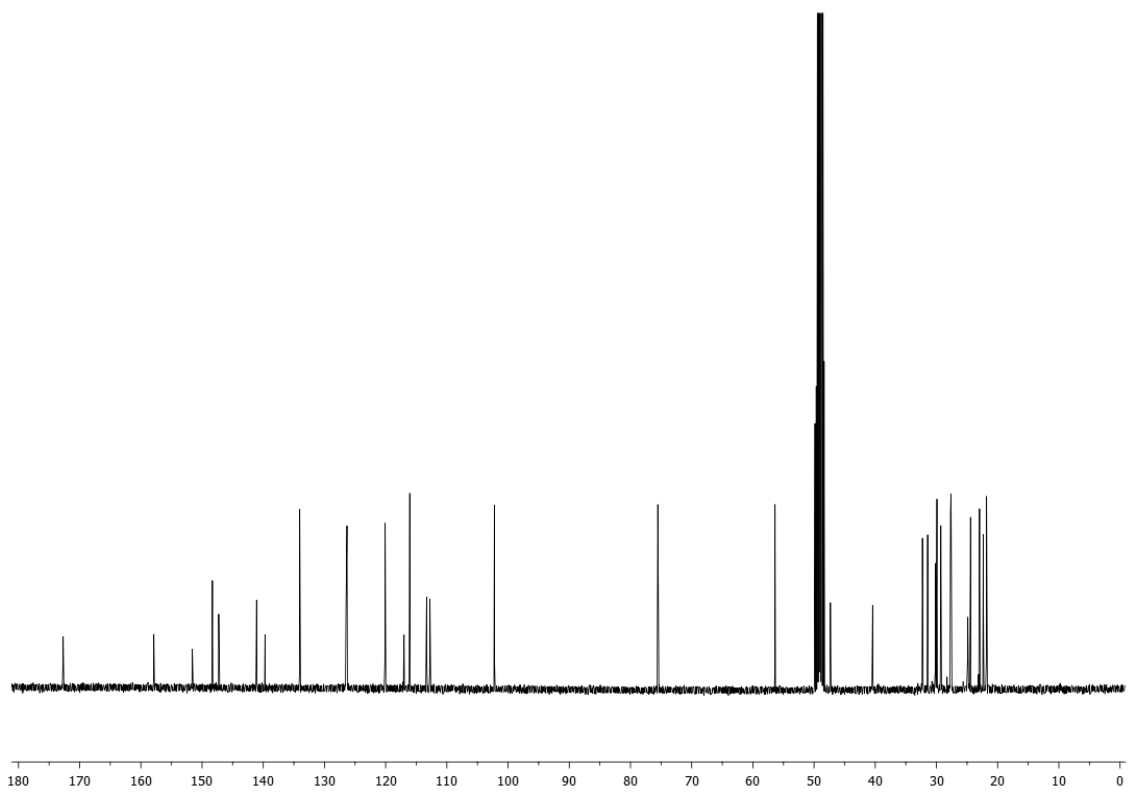
N-{6-[*(6-Chloro-1,2,3,4-tetrahydroacridin-9-yl)amino*]hexyl}-2-(6-benzyloxy-7-methoxy-2-methylchroman-2-yl)acetamide (**11e**)



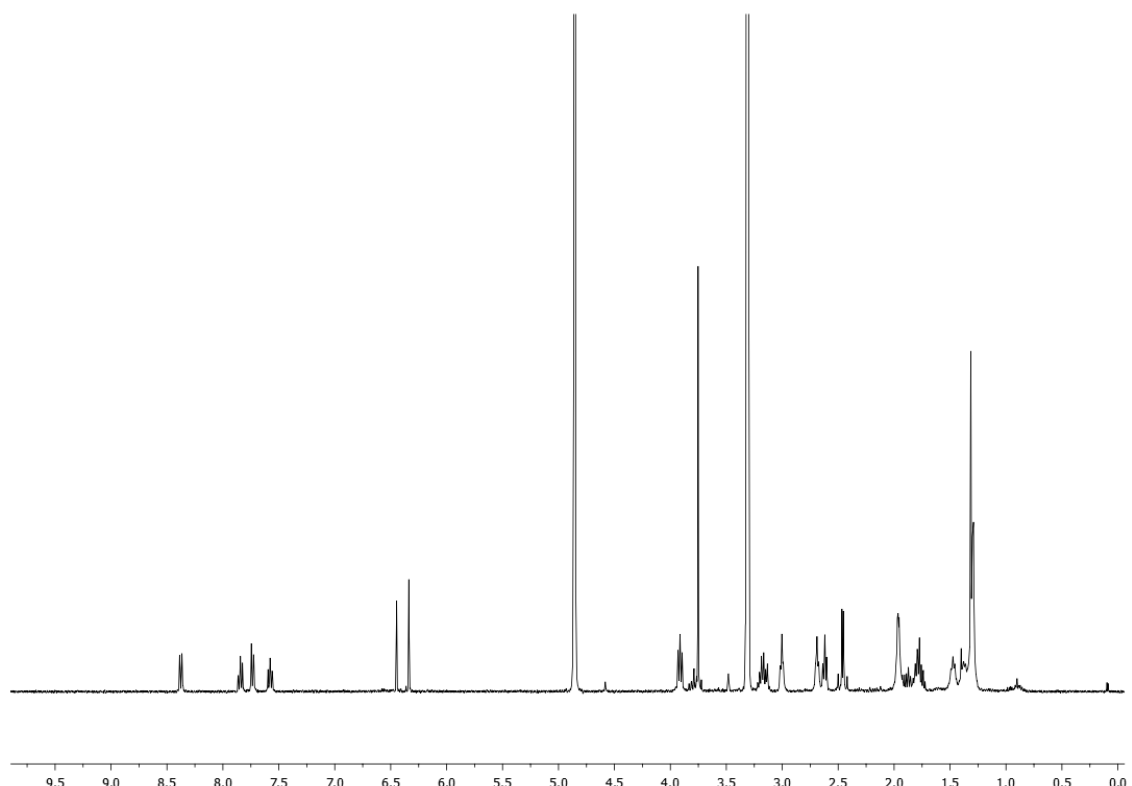
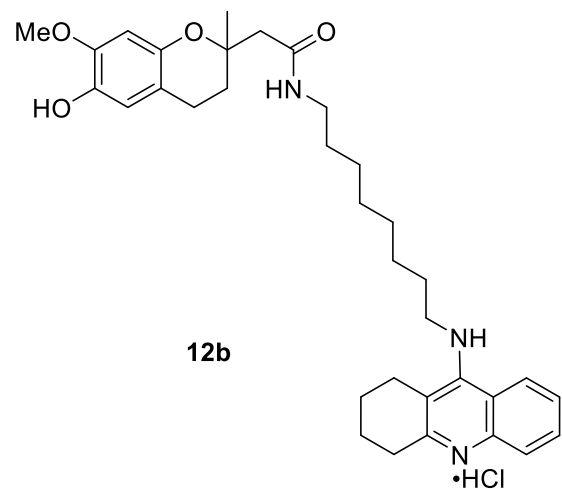


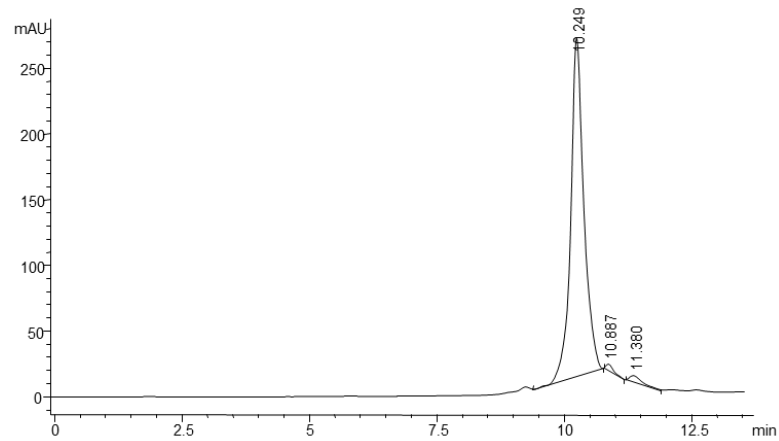
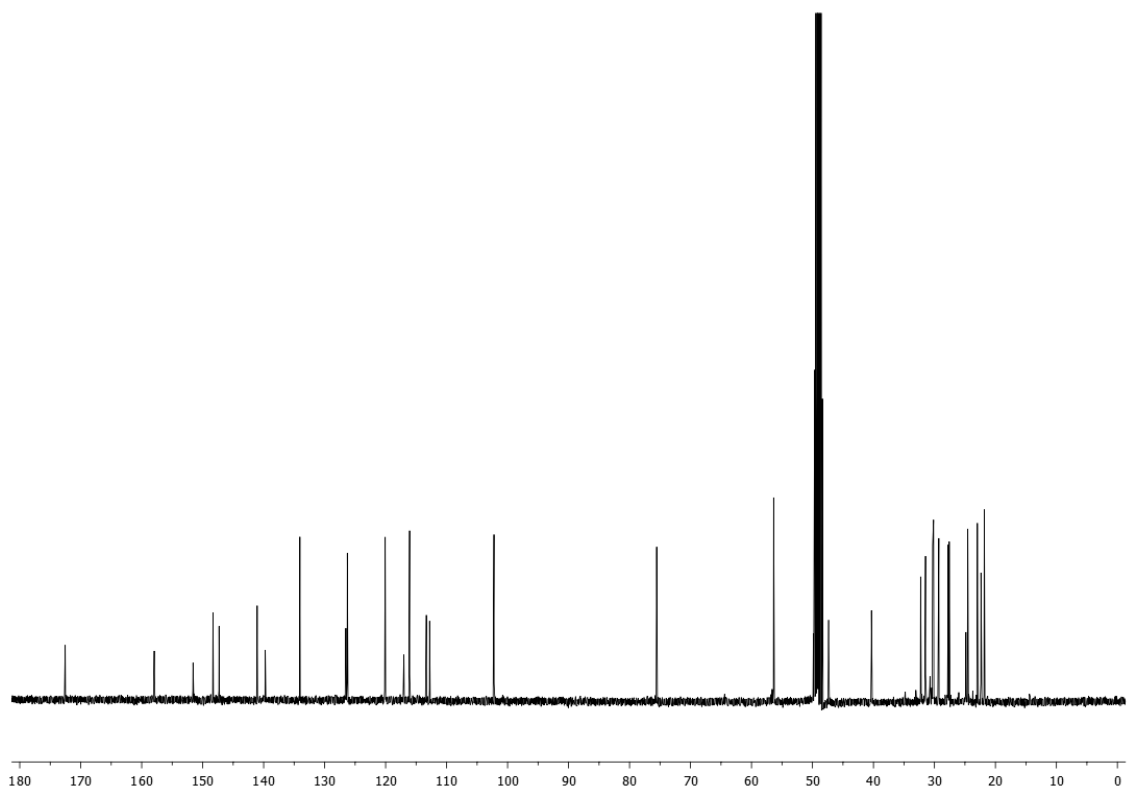
N-{7-[*(*1,2,3,4-Tetrahydroacridin-9-yl)amino]heptyl}-2-(6-hydroxy-7-methoxy-2-methylchroman-2-yl)acetamide (**12a**)



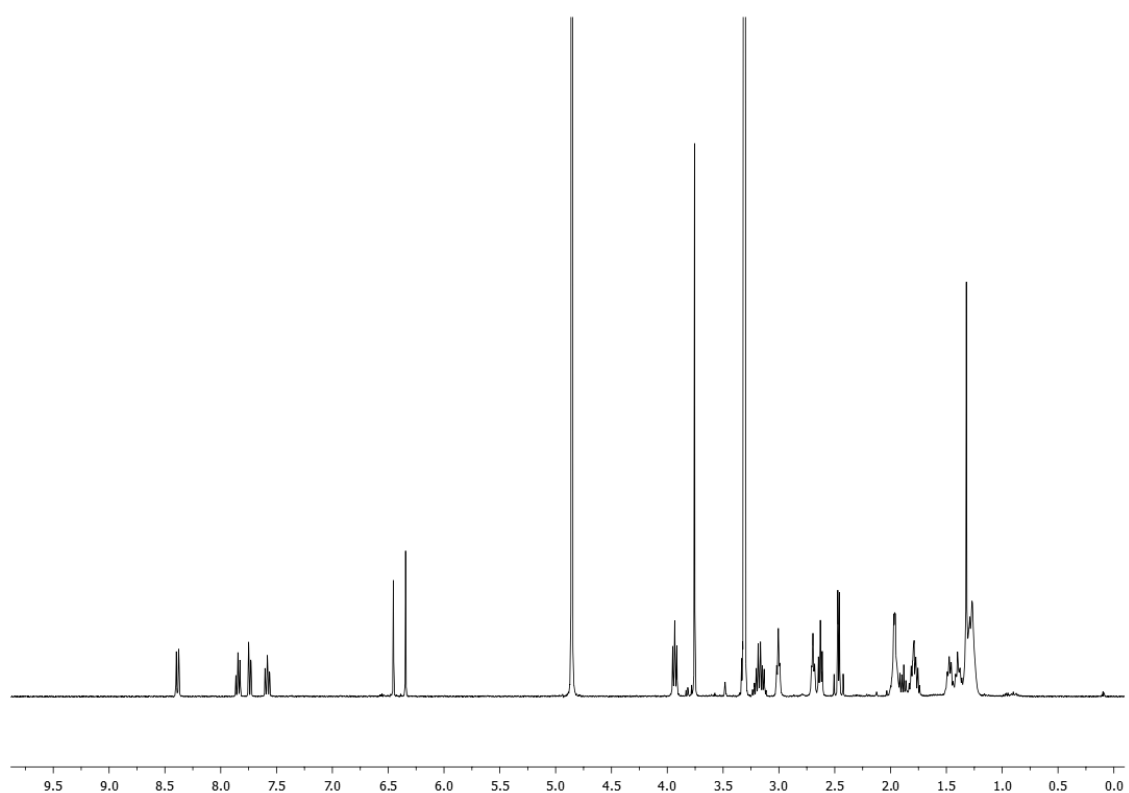
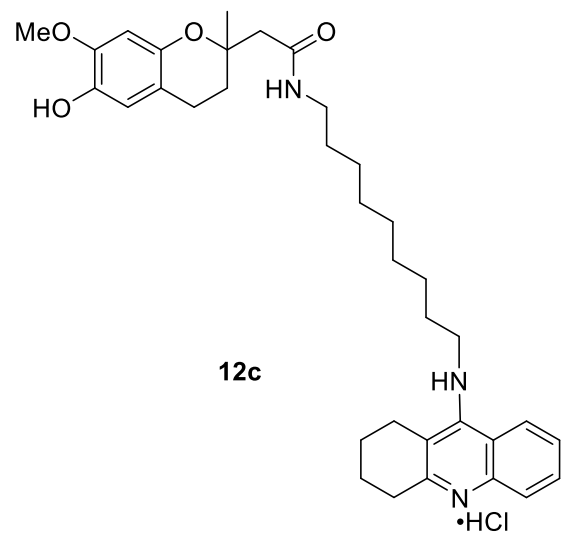


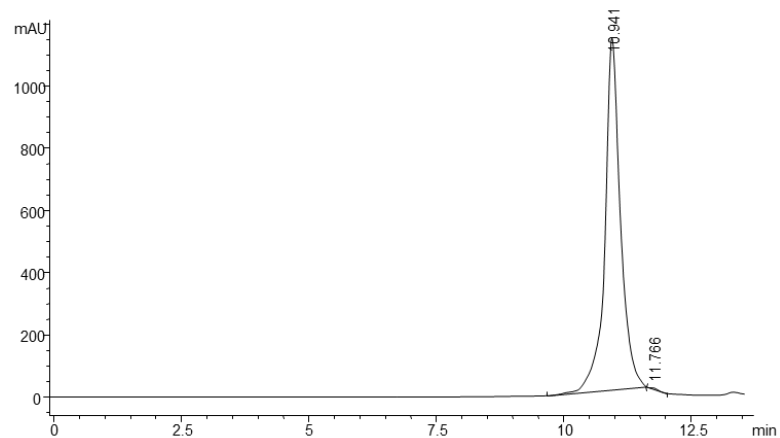
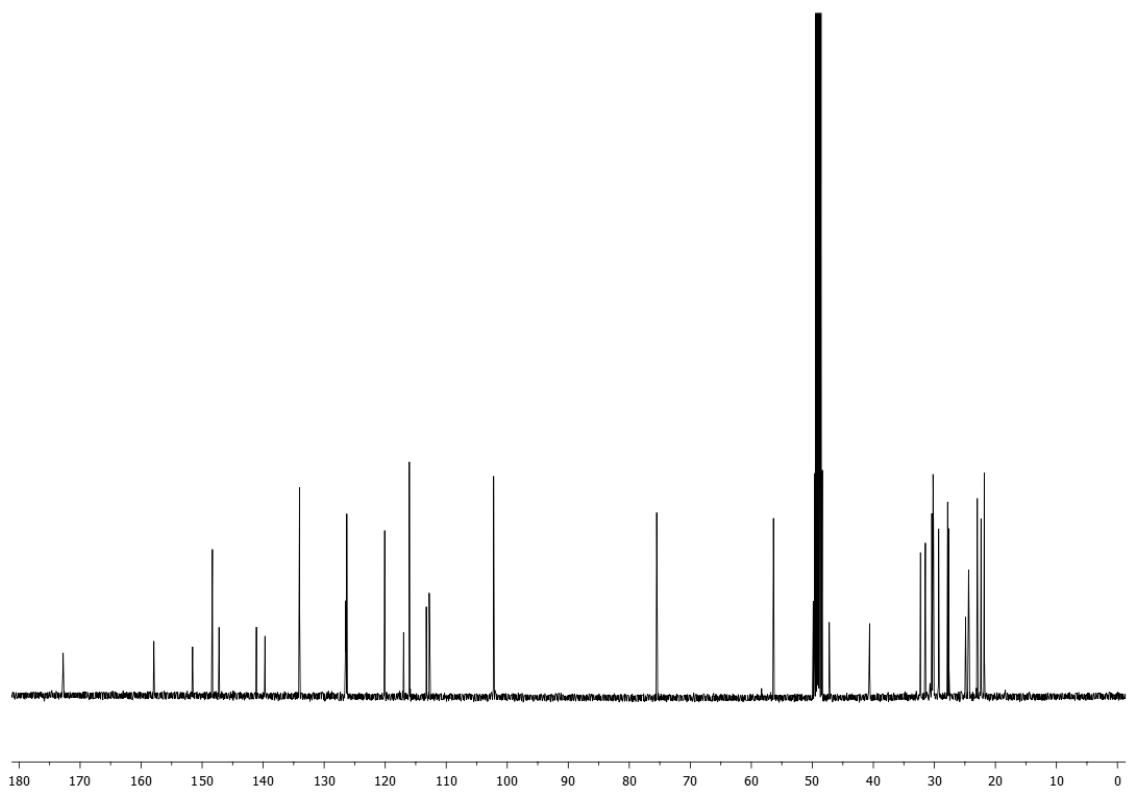
N-{8-[*(*1,2,3,4-Tetrahydroacridin-9-yl)amino]octyl}-2-(6-hydroxy-7-methoxy-2-methylchroman-2-yl)acetamide (**12b**)





N-(9-((1,2,3,4-Tetrahydroacridin-9-yl)amino)nonyl)-2-(6-hydroxy-7-methoxy-2-methylchroman-2-yl)acetamide (**12c**)





N-{6-[*(*1,2,3,4-Tetrahydroacridin-9-yl)amino]hexyl}-2-(6-hydroxy-7-methoxy-2-methylchroman-2-yl)acetamide (**12e**)

